Nonlinear Acoustics in a Viscothermal Boundary Layer over an Acoustic Lining*

Owen D. Petrie†
DAMTP, University of Cambridge, Cambridge CB3 0WA, United Kingdom

Edward J. Brambley‡
Mathematics Institute and WMG, University of Warwick, Coventry CV4 7AL, United Kingdom

Sound within aircraft engines can be 120dB–160dB, pushing the validity of linearized governing equations. Moreover, some components of sound within a visco-thermal mean flow boundary layer over an acoustic lining may be amplified by a factor of ~ 100 ($\sim 40\,\mathrm{dB}$) in a typical aircraft engine compared with the sound outside the boundary layer, which may be expected to trigger nonlinear effects within the boundary layer. This is in addition to the well-known nonlinear effects within the holes of the perforated lining facing sheet. This paper presents a mathematical investigation into the effects of weak nonlinearity on the acoustics within a thin parallel mean flow boundary layer in flow over an acoustic lining in a cylindrical duct. (This is the first investigation of nonlinear acoustics in a boundary layer flow over a non-rigid surface, to our knowledge.) In certain cases, a surprisingly large acoustic streaming effect is found that escapes the mean flow boundary layer and pervades well out into the interior of the duct.

I. Introduction

Acoustic liners are an essential part of civilian aircraft engines, enabling them to meet ever stricter noise requirements. Sound within aircraft engines is loud, potentially 120dB–160dB or more, pushing the validity of the usual assumption of linearised sound over a steady mean background flow. Moreover, a thin visco-thermal mean flow boundary layer of thickness δ^* over an acoustic lining was recently predicted [2] to give an amplification by a factor of order λ^*/δ^* to certain elements of the acoustic solution, where λ^* is a typical wavelength. Since typically $\lambda^*/\delta^* \approx 100$ for aeroengine intakes, even when the sound within the intake may validly be considered linear, nonlinear effects would be expected within the mean flow boundary layers over acoustic linings owing to this amplification. Experimental evidence also suggests nonlinearity becomes important at lower amplitudes than might otherwise be expected for flow over an acoustic lining [3]. This is a separate effect to the nonlinearities that occur within acoustic linings [e.g. 4]. Here, the effects of nonlinearities within thin mean flow boundary layers are investigated by mathematically modelling weakly nonlinear acoustics in a visco-thermal boundary layer flow over an acoustic lining in a cylindrical duct.

Acoustic linings are typically modelled as an array of Helmholtz resonators. Assuming a linear response, the effect of the acoustic lining is reduced to an impedance boundary condition, which is a linear relation between the acoustic pressure $\mathrm{Re}\big(\hat{p}\exp\{\mathrm{i}\omega t - \mathrm{i}kx - \mathrm{i}m\theta\}\big)$ and the acoustic normal velocity $\mathrm{Re}\big(\hat{v}\exp\{\mathrm{i}\omega t - \mathrm{i}kx - \mathrm{i}m\theta\}\big)$ at the boundary, $\hat{p} = Z\hat{v}$, where Z is typically a function of the frequency ω. Singh and Rienstra [4] showed that nonlinearity is generally unimportant for frequencies away from the resonant frequencies of the resonators, but that near the resonant frequencies the impedance needs to be modified to include a nonlinear term due to the inertia of the fluid in the resonator necks. Other authors have considered introducing nonlinearity by making the impedance Z depend on the wave amplitude as well as the frequency [e.g. 5]. It is again emphasized that the current study investigates the effects of nonlinearity in the mean flow boundary layer above the lining, not in the lining itself, and so is complementary to these other studies.

Much of the work on acoustics in flow over acoustic linings uses the Myers [6] boundary condition, $\frac{\hat{p}}{\hat{v}} = Z_{\mathrm{eff}} = \frac{\omega Z}{\omega - Uk}$, where Z is the actual boundary impedance and Z_{eff} is the effective boundary impedance seen by the acoustics in a uniform mean flow of velocity U within the duct. This comes from matching the normal fluid displacement at the

*A preliminary version of this work [1] was presented as AIAA Paper 2017-3376 at the 23rd AIAA/CEAS Aeroacoustics conference, 5–9 June 2017, in Denver, CO, USA.

†PhD student, DAMTP, CMS, Wilberforce Road, Cambridge CB3 0WA, United Kingdom. AIAA student member.

‡Associate Professor and Royal Society University Research Fellow, Mathematics Institute and WMG, University of Warwick, Coventry CV4 7AL, United Kingdom. AIAA senior member.

boundary, and is correct for thin mean flow boundary layers, either at high frequencies [2, 7] or for inviscid flows [8, 9]. Rienstra [10] showed that the Myers boundary condition leads not only to the expected acoustic modes, but also to surface modes that exist predominantly near the wall of the duct, one of which he categorized as a hydrodynamic instability; the presence of instabilities which grow in amplitude is another reason to consider nonlinear effects. However, the Myers boundary condition implies an infinitely thin mean flow boundary layer at the lining, and not only do boundary layers need to be extremely thin for this to be accurate [8, 9], but it also causes the Myers boundary condition to be ill-posed [11]. More recent work [12] gave a modified Myers boundary condition which accounted for the thin boundary layer of the mean flow, but still ignored the effect of viscosity. However, Renou and Auregan [13] demonstrated that to correlate mathematical and numerical results with the results of experiments, the effect of viscosity within the mean flow boundary layer must be included, and Khamis and Brambley [14, 15] demonstrated that the effects of viscosity on the acoustics are of a comparable magnitude to the effects of shear, and thus both should be taken into account. Viscosity within the mean flow boundary layer was investigated by Aurégan, Starobinski, and Pagneux [7] for thin low-velocity mean flow boundary layers, and by Brambley [2] for thin mean flow boundary layers of arbitrary subsonic velocity, while investigations taking into account both shear and viscosity within the mean flow boundary layer have recently been performed by Khamis and Brambley [16, 17]. This approach agrees most closely with results from solving the linearised Navier Stokes equations (LNSE) for the entire duct. The aim of all this work has been to derive a new boundary condition in terms of an effective impedance Z_{eff} as a function of the actual wall impedance Z. This is the impedance that sound in an inviscid uniform mean flow would observe at the boundary, and includes the effects of the viscous mean flow boundary layer. None of these studies have considered nonlinearity of the acoustics within the fluid.

Several studies have considered nonlinearity within mean flow boundary layers over rigid non-deformable surface [e.g. 18–20], or surfaces where the motion of the surface is known a priori and does not react to the acoustics [e.g. 21]. For example, Dong and Wu [19] considered free stream vortical disturbances to the Orr-Sommerfeld/Squire equations for an incompressible mean flow boundary layer and also found an amplification in the streamwise velocity; however, they deemed such solutions to be non-physical due to "entanglement of Fourier components". This work has subsequently been generalized to compressible flows [22]. Wu [21] derived effective impedances accounting for the effect of the mean flow boundary layer on perturbations to several non-reacting surfaces, where the behaviour of the surface is given a priori and does not react to the perturbation. However, the asymptotic scaling is significantly different between these non-reacting walls and the reacting lined walls considered here, and in particular the amplification by a factor of λ^*/δ^* mentioned above does not occur with non-reacting walls.

In this paper, the effect of nonlinearity in sound in a mean flow boundary layer above a non-rigid lined wall is considered. We restrict ourselves to the weakly nonlinear regime $|\tilde{v}|/\omega \ll \delta^* \ll \ell^*$, where ℓ^* is the duct radius; that is, the acoustic displacement is much smaller than the mean flow boundary layer thickness, and the mean flow boundary layer thickness is much smaller than the duct radius. In this regime, the linearised results are reproduced at leading order, while nonlinear effects occur as higher order corrections. This is compatible with nonlinear impedance models, and is a similar scaling to that used by Singh and Rienstra [4] away from resonance. We will not look at the stability and nonlinear effects of surface modes, however the analysis presented here could be used in the future to carry out such an investigation. After setting out the governing equations and nondimensionalization used here in section II and the mean flow used in section III, the asymptotic expansion used for weakly nonlinear perturbations to a thin mean flow boundary layer is presented in section IV. This is then solved, first for the linear acoustics in section IV.A, and then for the next order nonlinear perturbation in section IV.B. Plots of the results of this analysis, compared with solutions to the Weakly Non-Linear Navier–Stokes Equations (WNLNSE), are given in section V, after which conclusions and opportunities for further research are discussed in section VI.

II. Governing Equations

We consider the acoustics in a compressible viscous perfect gas inside a cylindrical duct, as depicted in figure 1. We non-dimensionalise all quantities as shown in table 1, giving the governing equations [23]

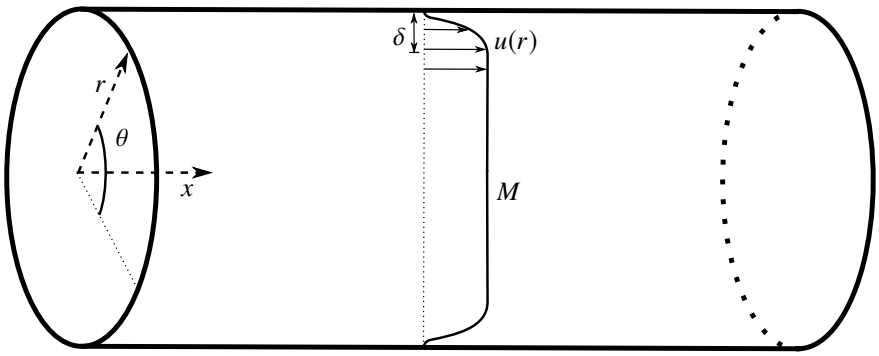

Fig. 1 Diagram of the duct

Density	$\rho^* = \rho_R^* \rho$	Pressure	$p^* = c_R^{*2} \rho_R^* p$
Velocity	$\mathbf{u}^* = c_R^* \mathbf{u}$	Viscosity	$\mu = c_R^* \ell^* \rho_R^* \mu$
Distance	$x^* = \ell^* x$	Thermal Conductivity	$\kappa^* = c_R^* \ell^* \rho_R^* c_p^* \kappa$
Time	$t^* = \ell^* / c_R^* t$	Temperature	$T^* = c_R^{*2} / c_p^* T$

Table 1 Dimensional and non-dimensional variables where $*$ denotes a dimensional variable, with reference lengthscale ℓ^*, reference velocity c_R^*, reference density ρ_R^*, and specific heat at constant pressure c_p^*.

$$\frac{\partial \rho}{\partial t} + \nabla \cdot (\rho \mathbf{u}) = 0 \tag{1a}$$

$$\rho \frac{D\mathbf{u}}{Dt} = -\nabla p + \nabla \cdot \sigma \tag{1b}$$

$$\sigma_{ij} = \mu \left(\frac{\partial u_i}{\partial x_j} + \frac{\partial u_j}{\partial x_i} \right) + \left(\mu^{\mathrm{B}} - \tfrac{2}{3}\mu \right) \delta_{ij} \nabla \cdot \mathbf{u} \tag{1c}$$

$$\rho \frac{DT}{Dt} = \frac{Dp}{Dt} + \nabla \cdot (\kappa \nabla T) + \sigma_{ij} \frac{\partial u_i}{\partial x_j} \tag{1d}$$

$$T = \tfrac{\gamma p}{(\gamma - 1)\rho} \tag{1e}$$

where $D/Dt = \partial/\partial t + \mathbf{u} \cdot \nabla$ and $\gamma = c_p^*/c_v^*$ is the ratio of specific heats. We assume that the viscosities and thermal conductivity depend linearly on the temperature and are independent of pressure [24],

$$\mu = \frac{T}{T_R \mathrm{Re}}, \qquad \mu^{\mathrm{B}} = \frac{T}{T_R \mathrm{Re}} \frac{\mu_R^{B^*}}{\mu_R^*}, \qquad \kappa = \frac{T}{T_R \mathrm{PrRe}}, \tag{2}$$

where $\mathrm{Re} = c_R^* \ell^* \rho_R^* / \mu_R^*$ is the Reynolds number based on the sound speed c_R^* and $\mathrm{Pr} = \mu_R^* c_p^* / \kappa_R^*$ is the Prandtl number. In the duct we use cylindrical coordinates (r^*, θ, x^*). We assume that the mean flow is uniform and time-independent and has a boundary layer thickness δ^*. We then take the reference values c_R^*, ρ_R^*, T_R^*, μ_R^*, $\mu_R^{B^*}$ and κ_R^* to be those of the uniform mean flow outside the boundary layer, and the reference lengthscale ℓ^* to be the duct radius. In non-dimensional terms, this gives the reference temperature $T_R = 1/(\gamma - 1)$ and the reference pressure $p_R = 1/\gamma$, while the duct wall is at $r = 1$; the non-dimensionalised uniform mean flow velocity $U_R = M$ is the Mach number. For air at sea level, $\rho_R^* \approx 1.225 \mathrm{kgm}^{-3}$, $c_R^* \approx 340 \mathrm{ms}^{-1}$, $\mu_R^* \approx 2 \times 10^{-5} \mathrm{Pa \cdot s}$, $c_p^* \approx 10^3 \mathrm{m}^2 \mathrm{s}^{-2} \mathrm{K}^{-1}$, and $\gamma = 1.4$. Taking $\ell^* \approx 1\mathrm{m}$ and a thin (perhaps laminar) boundary layer of $\delta^* \approx 1\mathrm{mm}$ then gives the order of magnitude estimates $\mathrm{Re} \approx 10^7$ and $\delta^*/\ell^* = \delta \approx 10^{-3}$, while a thicker (perhaps turbulent) boundary layer of $\delta^* \approx 1\mathrm{cm}$ would give $\delta \approx 10^{-2}$.

An acoustic perturbation is a small amplitude perturbation of magnitude ε to an otherwise steady mean flow. Here we specify ε explicitly as the nondimensionalized root mean square pressure oscillation, $p_{\mathrm{rms}}^* = \rho_R^* c_R^{*2} \varepsilon$. This is often given as a Sound Pressure Levels in deciBels, which at sea level is given by

$$\mathrm{SPL} = 20 \log_{10} \left(\frac{p_{\mathrm{rms}}^*}{2 \times 10^{-5}\,\mathrm{Pa}} \right) \approx 197 + 20 \log_{10} \varepsilon. \tag{3}$$

For sound pressure levels between 120dB and 160dB, we find ε has an order of magnitude varying between 1.4×10^{-4} and 1.4×10^{-2}. For the subsequent weakly nonlinear approximation to be valid, we will require $\varepsilon \ll \delta$.

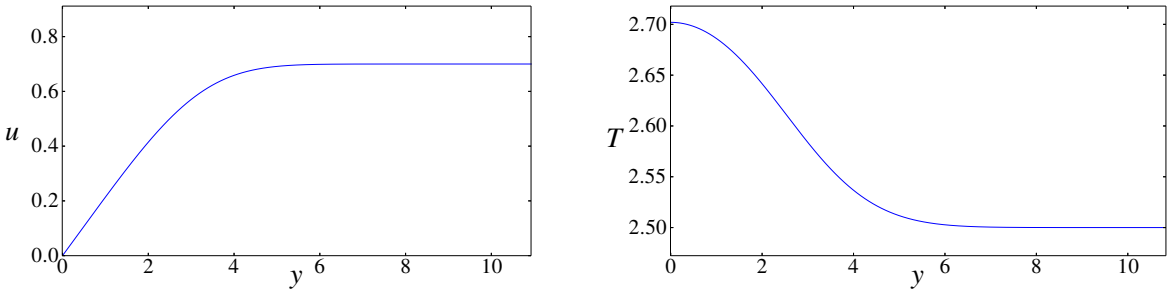

Fig. 2 Boundary Layer Profile (u left, T right) for $M = 0.7$, Pr $= 0.7$, $\xi = 1$ and $\delta = 10^{-3}$

III. Mean Flow

At the duct wall $r = 1$ we consider a steady thin boundary layer of thickness δ. Since the boundary layer is characterised by balancing viscous shear with inertia, inside the boundary layer we use the scalings

$$r = 1 - \delta y, \qquad \xi\delta^2 = 1/\mathrm{Re} \tag{4}$$

where ξ is a parameter adjusting how well developed the boundary layer is, and we assume here $\xi \sim O(1)$. The mean flow boundary layer is then given by

$$\boldsymbol{u} = u_0(y)\boldsymbol{e_x}, \qquad T = T_0(y), \qquad \rho = \rho_0(y), \qquad \text{and} \qquad p = 1/\gamma. \tag{5}$$

Any parallel non-swirling boundary layer profile could be used for what follows, provided it is independent of t, x and θ and is in thermal equilibrium with the boundary, meaning $\mathrm{d}T_0/\mathrm{d}y = 0$ at $y = 0$. Examples common in aeroacoustics include parabolic, $1/7$th power law, logarithmic and exponential boundary layer profiles. For the results given here, a parallel non-developing compressible Blasius boundary layer is used, as was used in [2]. This profile is given by

$$u_0 = M\frac{\mathrm{d}f}{\mathrm{d}\zeta}, \qquad \frac{1}{(\gamma-1)\rho_0} = T_0 = \frac{1}{\gamma-1} + \frac{1}{2}M^2\tau(\zeta), \qquad y = \frac{1}{\sqrt{M}}\int_0^\zeta 1 + \frac{(\gamma-1)}{2}M^2\tau(q)\mathrm{dq}, \tag{6}$$

where

$$ff'' + 2f''' = 0, \qquad \tau' = -2\mathrm{Pr}\,(f'')^{\mathrm{Pr}}\int_0^\zeta (f''(q))^{2-\mathrm{Pr}}\mathrm{dq}, \tag{7}$$

with boundary conditions

$$f(0) = f'(0) = 0, \qquad f' \to 1 \quad \text{as} \quad \zeta \to \infty, \qquad \tau \to 0 \quad \text{as} \quad \zeta \to \infty. \tag{8}$$

These equations are solved numerically, and an example is plotted in figure 2. As was pointed out in [2], it is only physically justifiable to take this Blasius boundary layer profile as being parallel (i.e. not spatially developing in x) if the region under consideration is far downstream for the duct entrance, which would correspond to $\xi \ll 1$ in the scalings above. Notwithstanding this, and since the analysis which follows is valid for an arbitrary parallel boundary layer profile, we shall not limit ourselves here to $\xi \ll 1$ but shall consider the general case $\xi = O(1)$.

IV. Acoustic Perturbations

Outside the mean flow boundary layer (i.e. within the duct away from the walls) we assume gradients are not large, so that the viscous terms, which are $O(1/\mathrm{Re}) = O(\delta^2)$ from (2), can be neglected. Writing all variables as $O(\varepsilon)$ time dependent perturbations to the steady mean flow,

$$\mathbf{u} = (M + \varepsilon\tilde{u}_O,\, \varepsilon\tilde{v}_O,\, \varepsilon\tilde{w}_O), \qquad p = 1/\gamma + \varepsilon\tilde{p}_O, \qquad \rho = 1 + \varepsilon\tilde{\rho}_O, \qquad \text{and} \qquad T = 1/(\gamma-1) + \varepsilon\tilde{T}_O, \tag{9}$$

the governing equations (1) become, with subscripts denoting differentiation,

$$\tilde{\rho}_{Ot} + M\tilde{\rho}_{Ox} + \tilde{u}_{Ox} + \tfrac{1}{r}(r\tilde{v}_O)_r + \tfrac{1}{r}\tilde{w}_{O\theta} = -\varepsilon\big[(\tilde{\rho}_O\tilde{u}_O)_x + \tfrac{1}{r}(r\tilde{\rho}_O\tilde{v}_O)_r + \tfrac{1}{r}(\tilde{\rho}_O\tilde{w}_O)_\theta\big] \tag{10a}$$

$$\tilde{u}_{Ot} + M\tilde{u}_{Ox} + \tilde{p}_{Ox} = -\varepsilon\big[\tilde{\rho}_O\tilde{u}_{Ot} + \tilde{\rho}_O M\tilde{u}_{Ox} + \tilde{u}_O\tilde{u}_{Ox} + \tilde{v}_O\tilde{u}_{Or} + \tfrac{1}{r}\tilde{w}_O\tilde{u}_{O\theta}\big] + O(\varepsilon^2) \tag{10b}$$

$$\tilde{v}_{Ot} + M\tilde{v}_{Ox} + \tilde{p}_{Or} = -\varepsilon\big[\tilde{\rho}_O\tilde{v}_{Ot} + \tilde{\rho}_O M\tilde{v}_{Ox} + \tilde{u}_O\tilde{v}_{Ox} + \tilde{v}_O\tilde{v}_{Or} + \tfrac{1}{r}\tilde{w}_O\tilde{v}_{O\theta} - \tfrac{1}{r}\tilde{w}_O\tilde{w}_O\big] + O(\varepsilon^2) \tag{10c}$$

$$\tilde{w}_{Ot} + M\tilde{w}_{Ox} + \frac{1}{r}\tilde{p}_{O\theta} = -\varepsilon\big[\tilde{\rho}_O\tilde{w}_{Ot} + \tilde{\rho}_O M\tilde{w}_{Ox} + \tilde{u}_O\tilde{w}_{Ox} + \tilde{v}_O\tilde{w}_{Or} + \tfrac{1}{r}\tilde{w}_O\tilde{w}_{O\theta} + \tfrac{1}{r}\tilde{v}_O\tilde{w}_O\big] + O(\varepsilon^2) \tag{10d}$$

$$\begin{aligned}\tilde{T}_{Ot} + M\tilde{T}_{Ox} - \tilde{p}_{Ot} - M\tilde{p}_{Ox} = -\varepsilon\big[&\tilde{\rho}_O\tilde{T}_{Ot} + \tilde{\rho}_O M\tilde{T}_{Ox} + \tilde{u}_O\tilde{T}_{Ox} + \tilde{v}_O\tilde{T}_{Or} + \tfrac{1}{r}\tilde{w}_O\tilde{T}_{O\theta} \\ &- \tilde{u}_O\tilde{p}_{Ox} - \tilde{v}_O\tilde{p}_{Or} - \tfrac{1}{r}\tilde{w}_O\tilde{p}_{O\theta}\big] + O(\varepsilon^2)\end{aligned} \tag{10e}$$

$$\gamma\tilde{p}_O - \tilde{\rho}_O - (\gamma-1)\tilde{T}_O = \varepsilon(\gamma-1)\tilde{T}_O\tilde{\rho}_O \tag{10f}$$

where we have used that the mean flow is constant with $u_0 = M$, $\rho_0 = 1$, $p_0 = 1/\gamma$ and $T_0 = 1/(\gamma-1)$. Equation (10f) may be used to eliminate $\tilde{\rho}_O$ from the other governing equations, $\tilde{\rho}_O = \gamma\tilde{p}_O - (\gamma-1)\tilde{T}_O - \varepsilon\gamma(\gamma-1)\tilde{T}_O\tilde{p}_O + \varepsilon(\gamma-1)^2\tilde{T}_O^2 + O(\varepsilon^2)$, leaving five equation (10a)–(10e) in the five unknowns $\tilde{p}_O$, $\tilde{T}_O$, $\tilde{u}_O$, $\tilde{v}_O$ and $\tilde{w}_O$. The order of magnitude of the terms in (10) suggest the asymptotic expansion

$$\tilde{T}_O = \tilde{T}_{O1} + \varepsilon\tilde{T}_{O2} + O\big(\varepsilon^2\big) \qquad \Rightarrow \qquad T = T_0 + \varepsilon\tilde{T}_{O1} + \varepsilon^2\tilde{T}_{O2} + O\big(\varepsilon^3\big), \tag{11}$$

and similarly for the other variables. The quantities labelled '1' are the leading order (linear) perturbations, while the quantities labelled '2' are the first order nonlinear corrections. Note that it will turn out later that some quantities labelled '2', for example $\tilde{v}_{O2}$, will be $O(1/\delta)$ from matching with the inner solution within the boundary layer, and will therefore give rise to an overall effect of magnitude $O(\varepsilon^2/\delta)$, larger than would otherwise be expected from ordinary weak nonlinearity. We will return to solving these equation in section IV.A.1.

Inside the mean flow boundary layer, we rescale using (4) and the leading order scaling from [2], giving

$$\mathbf{u} = \big(u_0 + \tfrac{\varepsilon}{\delta}\tilde{u},\, -\varepsilon\tilde{v},\, \varepsilon\tilde{w}\big), \qquad p = 1/\gamma + \varepsilon\tilde{p} \qquad \rho = \rho_0 + \tfrac{\varepsilon}{\delta}\tilde{\rho}, \qquad \text{and} \qquad T = T_0 + \tfrac{\varepsilon}{\delta}\tilde{T}. \tag{12}$$

Note that $\tilde{u}$, $\tilde{\rho}$ and $\tilde{T}$ give contributions that are a factor $1/\delta$ larger than in the outer scaling; this is in order to balance at leading order once we rescale into the boundary layer [see, e.g. 2], as will be seen below. The additional minus sign in front of $\tilde{v}$ in (12) is for convenience, meaning that $\tilde{v}$ is positive in the positive y-direction, while $\tilde{v}_O$ is positive in the positive r-direction. Substituting this into the governing equations (1) and expanding in powers of ε and δ leads to

$$\frac{\varepsilon}{\delta}\big[\tilde{\rho}_t + u_0\tilde{\rho}_x + \rho_0\tilde{u}_x + (\rho_0\tilde{v})_y\big] + \frac{\varepsilon^2}{\delta^2}\big[(\tilde{\rho}\tilde{u})_x + (\tilde{\rho}\tilde{v})_y\big] + \varepsilon\big[\rho_0\tilde{w}_\theta - \rho_0\tilde{v}\big] = O\left(\frac{\varepsilon^2}{\delta}, \varepsilon\delta\right) \tag{13a}$$

$$\begin{aligned}&\frac{\varepsilon}{\delta}\big[\rho_0\tilde{u}_t + \rho_0 u_0\tilde{u}_x + \rho_0 u_{0y}\tilde{v} - \xi(\gamma-1)(\tilde{T}u_{0y} + T_0\tilde{u}_y)_y\big] \\ &\quad + \frac{\varepsilon^2}{\delta^2}\big[\tilde{\rho}\tilde{u}_t + \tilde{\rho}u_0\tilde{u}_x + \tilde{\rho}\tilde{v}u_{0y} + \rho_0\tilde{u}\tilde{u}_x + \rho_0\tilde{v}\tilde{u}_y - \xi(\gamma-1)(\tilde{T}\tilde{u}_y)_y\big] \\ &\quad + \varepsilon\big[\xi(\gamma-1)[\tilde{T}u_{0y} + T_0\tilde{u}_y] + \tilde{p}_x\big] = O\left(\frac{\varepsilon^3}{\delta^3}, \frac{\varepsilon^2}{\delta}, \varepsilon\delta\right)\end{aligned} \tag{13b}$$

$$\begin{aligned}\frac{\varepsilon}{\delta}\tilde{p}_y = \varepsilon&\left[-\rho_0(\tilde{v}_t + u_0\tilde{v}_x) + \xi(\gamma-1)[\tilde{T}u_{0y} + T_0\tilde{u}_y]_x + \xi(\gamma-1)\left[2T_0\tilde{v}_y + \left(\frac{\mu_0^{B^*}}{\mu_0^*} - \frac{2}{3}\right)T_0(\tilde{v}_y + \tilde{u}_x)\right]_y\right] \\ &+ O\left(\frac{\varepsilon^3}{\delta^2}, \frac{\varepsilon^2}{\delta}, \varepsilon\delta\right)\end{aligned} \tag{13c}$$

$$\varepsilon\left[\rho_0\tilde{w}_t + \rho_0 u_0\tilde{w}_x + \tilde{p}_\theta - \xi(\gamma-1)(T_0\tilde{w}_y)_y\right] = O\left(\frac{\varepsilon^3}{\delta^2}, \frac{\varepsilon^2}{\delta}, \varepsilon\delta\right) \tag{13d}$$

$$\frac{\varepsilon}{\delta}\left[\rho_0\tilde{T}_t + \rho_0 u_0\tilde{T}_x + \rho_0\tilde{v}T_{0y} - \frac{\xi(\gamma-1)}{Pr}(T_0\tilde{T})_{yy} - \xi(\gamma-1)(\tilde{T}u_{0y}^2 + 2T_0u_{0y}\tilde{u}_y)\right]$$
$$+\frac{\varepsilon^2}{\delta^2}\left[\rho_0\tilde{u}\tilde{T}_x + \rho_0\tilde{v}\tilde{T}_y + \tilde{\rho}\tilde{T}_t + \tilde{\rho}u_0\tilde{T}_x + \tilde{\rho}\tilde{v}T_{0y} - \frac{\xi(\gamma-1)}{Pr}(\tilde{T}\tilde{T}_y)_y - \xi(\gamma-1)(T_0\tilde{u}_y^2 + 2\tilde{T}u_{0y}\tilde{u}_y)\right] \tag{13e}$$
$$-\varepsilon\left[\tilde{p}_t - u_0\tilde{p}_x + \frac{\xi(\gamma-1)}{Pr}(T_0\tilde{T})_y\right] = O\left(\frac{\varepsilon^3}{\delta^3}, \frac{\varepsilon^2}{\delta}, \varepsilon\delta\right)$$

$$\frac{\varepsilon}{\delta}\left[T_0\tilde{\rho} + \tilde{T}\rho_0\right] + \frac{\varepsilon^2}{\delta^2}\tilde{T}\tilde{\rho} - \varepsilon\frac{\gamma}{\gamma-1}\tilde{p} = 0 \tag{13f}$$

As before, (13f) may be used to eliminate $\tilde{\rho}$ from the other governing equations,

$$\tilde{\rho} = -\frac{\rho_0}{T_0}\tilde{T} + \delta\frac{\gamma}{(\gamma-1)T_0}\tilde{p} + \frac{\varepsilon}{\delta}\frac{\rho_0}{T_0^2}\tilde{T}^2 - \varepsilon\frac{\gamma}{(\gamma-1)T_0^2}\tilde{T}\tilde{p} + O(\delta^2), \tag{14}$$

leaving five equation (13a)–(13e) in the five unknowns $\tilde{p}$, $\tilde{T}$, $\tilde{u}$, $\tilde{v}$ and $\tilde{w}$. The order of magnitude of the terms in (13) suggest the expansion

$$\tilde{T} = \tilde{T}_1 + \frac{\varepsilon}{\delta}\tilde{T}_2 + \delta\tilde{T}_3 + O\left(\frac{\varepsilon^2}{\delta^2}, \varepsilon, \delta^2\right), \qquad \Rightarrow \qquad T = T_0 + \frac{\varepsilon}{\delta}\tilde{T}_1 + \frac{\varepsilon^2}{\delta^2}\tilde{T}_2 + \varepsilon\tilde{T}_3 + O\left(\frac{\varepsilon^3}{\delta^3}, \frac{\varepsilon^2}{\delta}, \varepsilon\delta\right) \tag{15a}$$

$$\tilde{u} = \tilde{u}_1 + \frac{\varepsilon}{\delta}\tilde{u}_2 + \delta\tilde{u}_3 + O\left(\frac{\varepsilon^2}{\delta^2}, \varepsilon, \delta^2\right), \qquad \Rightarrow \qquad \mathbf{u}\cdot\mathbf{e_x} = u_0 + \frac{\varepsilon}{\delta}\tilde{u}_1 + \frac{\varepsilon^2}{\delta^2}\tilde{u}_2 + \varepsilon\tilde{u}_3 + O\left(\frac{\varepsilon^3}{\delta^3}, \frac{\varepsilon^2}{\delta}, \varepsilon\delta\right) \tag{15b}$$

$$\tilde{v} = \tilde{v}_1 + \frac{\varepsilon}{\delta}\tilde{v}_2 + \delta\tilde{v}_3 + O\left(\frac{\varepsilon^2}{\delta^2}, \varepsilon, \delta^2\right), \qquad \Rightarrow \qquad \mathbf{u}\cdot\mathbf{e_r} = -\varepsilon\tilde{v}_1 - \frac{\varepsilon^2}{\delta}\tilde{v}_2 - \varepsilon\delta\tilde{v}_3 + O\left(\frac{\varepsilon^3}{\delta^2}, \varepsilon^2, \varepsilon\delta^2\right) \tag{15c}$$

$$\tilde{w} = \tilde{w}_1 + \frac{\varepsilon}{\delta}\tilde{w}_2 + \delta\tilde{w}_3 + O\left(\frac{\varepsilon^2}{\delta^2}, \varepsilon, \delta^2\right), \qquad \Rightarrow \qquad \mathbf{u}\cdot\mathbf{e}_\theta = \varepsilon\tilde{w}_1 + \frac{\varepsilon^2}{\delta}\tilde{w}_2 + \varepsilon\delta\tilde{w}_3 + O\left(\frac{\varepsilon^3}{\delta^2}, \varepsilon^2, \varepsilon\delta^2\right) \tag{15d}$$

$$\tilde{p} = \tilde{p}_1 + \frac{\varepsilon}{\delta}\tilde{p}_2 + \delta\tilde{p}_3 + O\left(\frac{\varepsilon^2}{\delta^2}, \varepsilon, \delta^2\right), \qquad \Rightarrow \qquad p = \frac{1}{\gamma} + \varepsilon\tilde{p}_1 + \frac{\varepsilon^2}{\delta}\tilde{p}_2 + \varepsilon\delta\tilde{p}_3 + O\left(\frac{\varepsilon^3}{\delta^2}, \varepsilon^2, \varepsilon\delta^2\right) \tag{15e}$$

The quantities labelled '1' are the leading order (linear) perturbations, quantities labelled '2' are the first order nonlinear correction, and quantities labelled '3' are the first order in δ linear correction (i.e. the first terms to involve mean flow shear). Note that we make no assumption about the relative size of ε/δ compared with δ, and so quantities labelled '3' should not be thought of as giving a smaller contribution than terms labelled '2', although both contributions are smaller than those from terms labelled '1'.

A. Linear acoustics

In this section we describe the process for solving the governing equations (10) and (13) with the asymptotic expansions (11) and (15) for the leading order linear terms (quantities labelled '1'), reproducing the results of [2]. A similar procedure can be used for the first order linear correction terms (quantities labelled '3'), as was done in [16]. We consider monochromatic perturbations, so that

$$\tilde{p}_{O1}(x, r, \theta, t) = \mathrm{Re}\Big(\hat{p}_{O1}(r)\exp\{\mathrm{i}\omega t - \mathrm{i}kx - \mathrm{i}m\theta\}\Big), \tag{16}$$

and similarly for the other linear variables. Here, ω is the frequency and k is the axial wavenumber, both of which will in general be complex, while m is the azimuthal wavenumber and is necessarily an integer. Since the equations we are working with here are linear, we do not have to take the real parts of the complex exponentials when substituting for the perturbations, and may instead work directly with the complex exponentials, as is usual in acoustics.

1. Outer solution in the duct interior

At leading order the governing equations (10) reduce to the standard Bessel equation for acoustics in a cylindrical duct. Applying the boundary condition that the solution is regular at $r = 0$, the solution for the pressure is given by

$$\hat{p}_{O1} = CJ_m(\alpha r) \qquad \text{where} \qquad \alpha^2 = (\omega - Mk)^2 - k^2, \tag{17}$$

and C is an arbitrary constant. The other quantities are then given in terms of $\hat{p}_{O1}$ by

$$\mathrm{i}(\omega - Mk)\hat{u}_{O1} - \mathrm{i}k\hat{p}_{O1} = 0, \tag{18a}$$

$$\mathrm{i}(\omega - Mk)\hat{v}_{O1} + \hat{p}_{O1r} = 0, \tag{18b}$$

$$\mathrm{i}(\omega - Mk)\hat{w}_{O1} - \mathrm{i}m\hat{p}_{O1}/r = 0, \tag{18c}$$

$$\hat{T}_{O1} = \hat{p}_{O1}. \tag{18d}$$

Since this solution is not valid within the mean flow boundary layer close to the wall, an inner solution that is valid in the mean flow boundary layer is needed.

2. Inner solution in the boundary layer

Inside the mean flow boundary layer, the expansion of the governing equations (13) at leading order, using the scalings in (15), gives

$$\mathcal{L}(\hat{u}_1, \hat{v}_1, \hat{T}_1; \omega, k) = \left\{ \begin{array}{c} \mathrm{i}(\omega - u_0 k)\hat{T}_1 + T_{0y}\hat{v}_1 - T_0\hat{v}_{1y} + \mathrm{i}kT_0\hat{u}_1 \\ \mathrm{i}(\omega - u_0 k)\hat{u}_1 + \hat{v}_1 u_{0y} - \xi(\gamma-1)^2 T_0(T_0\hat{u}_{1y} + \hat{T}_1 u_{0y})_y \\ \mathrm{i}(\omega - u_0 k)\hat{T}_1 + \hat{v}_1 T_{0y} - \xi(\gamma-1)^2 T_0\left[\frac{1}{Pr}(\hat{T}_1 T_0)_{yy} + \hat{T}_1(u_{0y})^2 + 2T_0 u_{0y}\hat{u}_{1y}\right] \end{array} \right\} = \mathbf{0} \tag{19a}$$

$$\hat{p}_{1y} = 0 \tag{19b}$$

where a subscript y denotes $\mathrm{d}/\mathrm{d}y$, giving a system of linear homogeneous ODEs in y. The boundary conditions at the wall ($y = 0$) are those of no slip ($\hat{u}_1 = 0$), thermal equilibrium ($\hat{T}_1 = 0$, obtained by assuming that the wall has a far higher thermal capacity than the fluid), and the impedance boundary condition $\hat{p}_1 = Z\hat{v}_1$, where $Z(\omega)$ is the known impedance of the boundary and is unrestricted apart from the assumption that it is independent of the wavenumbers k and m. Note that $\hat{p}_{1y} = 0$ implies that $\hat{p}_1$ is constant through the boundary layer, and so $\hat{p}_1(0) = \hat{p}_{O1}(1)$. Since the system of equations $\mathcal{L}$ is second order in $\hat{u}$ and $\hat{T}$, one further boundary condition on each of $\hat{u}$ and $\hat{T}$ is needed, which is obtained by requiring the inner solution to be compatible with an outer solution as $y \to \infty$. Finding a compatible outer solution to match to the inner solution is considered next.

3. Matching the outer and inner solutions

Sufficiently far outside the mean flow boundary layer for $y \geq Y \gg 1$, the gradients of the mean flow quantities vanish and the mean flow quantities attain their uniform mean flow values. Hence, for $y \geq Y$ the system of ODEs (19) decouples and becomes:

$$\mathcal{L}(\hat{u}_1, \hat{v}_1, \hat{T}_1; \omega, k) = \left\{ \begin{array}{c} \eta_\infty^2 \xi\hat{T}_1 - \frac{1}{(\gamma-1)}\hat{v}_{1y} + \frac{\mathrm{i}k}{(\gamma-1)}\hat{u}_1 \\ \eta_\infty^2\hat{u}_1 - \hat{u}_{1yy} \\ \eta_\infty^2\hat{T}_1 - \frac{1}{\sigma^2}\hat{T}_{1yy} \end{array} \right\} = \mathbf{0} \tag{20}$$

where $\sigma^2 = \mathrm{Pr}$ is the Prandtl number and $\eta_\infty^2 = \mathrm{i}(\omega - Mk)/\xi$ with $\mathrm{Re}(\eta_\infty) > 0$. This can now be solved analytically. The second and third equations have solutions which exponentially grow or decay as $y \to \infty$, and in order to match to an outer solution in the main part of the duct, only the decaying solutions are allowed. This leads to the boundary conditions at $y = Y$

$$\hat{u}_{1y} + \eta_\infty\hat{u}_1 = 0, \qquad \hat{v}_1 = \hat{v}_{1\infty} - \frac{\eta_\infty(\gamma-1)\xi}{\sigma}\hat{T}_1 - \frac{\mathrm{i}k}{\eta_\infty}\hat{u}_1, \qquad \hat{T}_{1y} + \sigma\eta_\infty\hat{T}_1 = 0 \qquad \text{at } y = Y, \tag{21}$$

where $\hat{v}_{1\infty} = \hat{v}_{O1}(1)$ is the radial velocity from the outer solution at the wall that the inner solution should match to.

In conclusion, solving (19) subject to the boundary conditions $\hat{T}_1 = 0$ and $\hat{u}_1 = 0$ at $y = 0$ and (21) at $y = Y$, where $\hat{v}_{1\infty}$ is given by (17) and (18) yields a unique solution. Requiring also the impedance boundary condition $\hat{p}_{O1}(1) = \hat{p}_1(0) = Z\hat{v}_1(0)$ at $y = 0$ gives a dispersion relation relating allowable values of k and ω. This gives the results of Brambley [2]. From the above, and the scalings given in (11) and (15), we note that the $O(\varepsilon)$ perturbations outside the boundary layer force $O(\varepsilon/\delta)$ perturbations within the mean flow boundary layer, but that these $O(\varepsilon/\delta)$ perturbations within the mean flow boundary layer do not propagate out of the mean flow boundary layer into the centre of the duct, where all terms remain $O(\varepsilon)$. This is because both $\hat{u}_1$ and $\hat{T}_1$ decay to zero outside the mean flow boundary

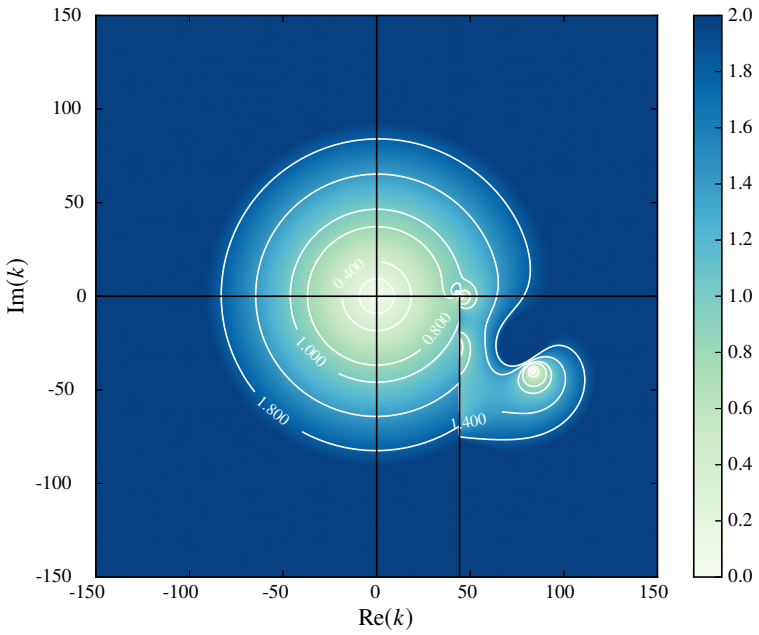

Fig. 3 Contour plot of $|1 - \frac{Z_{\text{eff}}}{Z/(1-\frac{Mk}{\omega})}|$ in the k-plane for $\omega = 31$, $M = 0.7$, $\delta = 10^{-3}$, Pr $= 0.7$ and $\xi = 1$, corresponding to Re $= 10^6$. The lighter shades are where the Myers condition agrees fairly closely with the viscous asymptotics whereas the darker shades are where the two schemes disagree.

layer. It should be noted that taking the decaying solution in (20) involves taking the correct branch of the square root of η_∞^2, so that $\mathrm{Re}(\eta_\infty) > 0$. This leads to a branch cut in the complex k-plane, with the branch point at $k = \omega/M$ and the branch cut extending vertically downwards towards $-\mathrm{i}\infty$. This branch cut can be seen prominently in figure 3, which plots $|1 - Z_{\text{eff}}/(1 - Mk/\omega)Z|$ in the k-plane for the leading order viscous asymptotics. Here, $Z_{\text{eff}} = \hat{p}_{O1}(1)/\hat{v}_{O1}(1)$ is the impedance the outer solution would see at the wall if it were not for the mean flow boundary layer, and therefore Z_{eff} includes the effect of both the liner and the mean flow boundary layer. Figure 3 therefore compares this effective impedance with the impedance from the Myers boundary condition, $Z/(1 - Mk/\omega)$.

For further details, including various asymptotic solutions of (19) in high- and low-frequency limits, the reader is referred to [2]. The same procedure as given here may be used to calculate the first order linear correction terms (quantities labelled '3' above), and such an analysis is given in [16]. Since these first order linear correction terms are not needed for calculating the nonlinear correction terms below, we do not reproduce this argument here. We now turn our attention to the nonlinear correction terms.

B. Nonlinear acoustics

We now solve for the nonlinear correction terms (quantities labelled '2' in equation 15). Substituting the asymptotic ansatz (15) into the governing equations (13) and taking terms quadratic in ε results in a set of linear ODEs to solve for the nonlinear correction terms, forced by terms quadratic in the leading order linear solution. Since these forcing terms are nonlinear, we must take care with the monochromatic assumption, by taking the real parts of the perturbed leading order quantities before multiplying. (Note that, in general, both ω and k may be complex, while m is an integer and so is necessarily real.) For example, the multiple of $\tilde{u}_1$ and $\mathrm{d}\tilde{v}_1/\mathrm{d}x$ is

$$\begin{aligned}\tilde{u}_1\frac{\mathrm{d}\tilde{v}_1}{\mathrm{d}x} &= \mathrm{Re}\big(\hat{u}_1\exp\{\mathrm{i}\omega t - \mathrm{i}kx - \mathrm{i}m\theta\}\big)\,\mathrm{Re}\big(-\mathrm{i}k\hat{v}_1\exp\{\mathrm{i}\omega t - \mathrm{i}kx - \mathrm{i}m\theta\}\big)\\ &= \frac{1}{2}\mathrm{Re}\Big(-\mathrm{i}k\hat{u}_1\hat{v}_1\exp\{2\mathrm{i}\omega t - 2\mathrm{i}kx - 2\mathrm{i}m\theta\} + \mathrm{i}k^\star\hat{u}_1\hat{v}_1^\star\exp\{\mathrm{i}(\omega-\omega^\star)t - \mathrm{i}(k-k^\star)x\}\Big), \quad (22)\end{aligned}$$

where a star denotes the complex conjugate. This therefore results in two different Fourier components: one of double the frequency $\Omega = 2\omega$ and double the axial wavenumber $K = 2k$ and azimuthal wavenumber $\mathcal{M} = 2m$ of the leading order acoustics; and a 'zero' frequency component that has the purely imaginary frequency $\Omega = \omega - \omega^\star$ and

wavenumber $K = k - k^\star$ and $\mathcal{M} = 0$. In either case, we write, e.g.,

$$\tilde{p}_{O2}(x, r, \theta, t) = \mathrm{Re}\Big(\hat{p}_{O2}(r)\exp\{\mathrm{i}\Omega t - \mathrm{i}Kx - \mathrm{i}\mathcal{M}\theta\}\Big), \tag{23}$$

and similarly for the other nonlinear variables.

1. Inner solution in the boundary layer

Substituting the scaling (15) into the governing equations (13) and equating terms of order ε^2/δ^2 gives the system of equations

$$\mathcal{L}(\hat{u}_2, \hat{v}_2, \hat{T}_2; \Omega, K) = \mathcal{Q}(\hat{u}_1, \hat{v}_1, \hat{T}_1; \hat{u}_1^\star, \hat{v}_1^\star, \hat{T}_1^\star; \omega, k), \tag{24a}$$

$$\hat{p}_{2y} = 0, \tag{24b}$$

where $\mathcal{L}$ is as given in (19). In the double frequency case, $\Omega = 2\omega$, $K = 2k$ and the $\star$ is ignored. In the 'zero' frequency case, $\Omega = \omega - \omega^\star$, $K = k - k^\star$ and the $\star$ denotes the complex conjugate. The forcing $\mathcal{Q}$ has the following form:

$$\mathcal{Q} = \begin{Bmatrix} \frac{T_{0y}}{T_0}(\hat{T}_1\hat{v}_1^\star) - \frac{1}{2}(\hat{T}_1\hat{v}_1^\star)_y + \frac{\hat{T}_1\hat{T}_1^\star}{2T_0}\mathrm{i}(\Omega - u_0K) + \frac{1}{2}\mathrm{i}K\hat{u}_1\hat{T}_1^\star \\ \frac{\mathrm{i}(\omega-u_0k)}{2T_0}(\hat{u}_1\hat{T}_1^\star) + \frac{\mathrm{i}k}{2}\hat{u}_1\hat{u}_1^\star + \frac{u_{0y}}{2T_0}(\hat{T}_1\hat{v}_1^\star) - \frac{1}{2}(\hat{v}_1\hat{u}_{1y}^\star) + \frac{\xi(\gamma-1)^2T_0}{2}(\hat{T}_1\hat{u}_{1y}^\star)_y \\ \frac{\mathrm{i}k}{2}(\hat{u}_1^\star\hat{T}_1) - \frac{1}{2}(\hat{v}_1\hat{T}_{1y}^\star) + \frac{\mathrm{i}(\omega-u_0k)}{2T_0}\hat{T}_1\hat{T}_1^\star + \frac{T_{0y}}{2T_0}(\hat{T}_1\hat{v}_1^\star) + \\ \qquad + \frac{\xi(\gamma-1)^2T_0}{2Pr}(\hat{T}_1^\star\hat{T}_{1y})_y + \frac{\xi(\gamma-1)^2T_0}{2}(T_0\hat{u}_{1y}\hat{u}_{1y}^\star + 2u_{0y}\hat{T}_1\hat{u}_{1y}^\star) \end{Bmatrix} \tag{25}$$

Similarly to the linear case, when the extrapolation outside the mean flow boundary layer at $y = Y \gg 1$ is carried out we get exponential terms $\propto \exp(\pm N_\infty y)$ where $N_\infty^2 = \mathrm{i}(\Omega - MK)/\xi$. The equations for large y are:

$$\begin{Bmatrix} N_\infty^2\xi\hat{T}_2 - \frac{1}{(\gamma-1)}\hat{v}_{2y} + \frac{\mathrm{i}K}{(\gamma-1)}\hat{u}_2 \\ N_\infty^2\xi\hat{u}_2 - \xi\hat{u}_{2yy} \\ N_\infty^2\xi\hat{T}_2 - \frac{\xi}{\sigma^2}\hat{T}_{2yy} \end{Bmatrix} = \begin{Bmatrix} -\frac{1}{2}(\hat{T}_1\hat{v}_1^\star)_y + \frac{\hat{T}_1\hat{T}_1^\star}{2T_0}\mathrm{i}(\Omega - MK) + \frac{1}{2}\mathrm{i}K\hat{u}_1\hat{T}_1^\star \\ \frac{\mathrm{i}(\omega-Mk)(\gamma-1)}{2}(\hat{u}_1\hat{T}_1^\star) + \frac{\mathrm{i}k}{2}\hat{u}_1\hat{u}_1^\star - \frac{1}{2}(\hat{v}_1\hat{u}_{1y}^\star) + \frac{\xi(\gamma-1)}{2}(\hat{T}_1\hat{u}_{1y}^\star)_y \\ \frac{\mathrm{i}k}{2}(\hat{u}_1^\star\hat{T}_1) - \frac{1}{2}(\hat{v}_1\hat{T}_{1y}^\star) + \frac{\mathrm{i}(\omega-Mk)(\gamma-1)}{2}\hat{T}_1\hat{T}_1^\star + \frac{\xi(\gamma-1)}{2Pr}(\hat{T}_1^\star\hat{T}_{1y})_y + \frac{\xi}{2}\hat{u}_{1y}\hat{u}_{1y}^\star \end{Bmatrix} \tag{26}$$

We have already shown that, for large y, $\hat{u}_1$ and $\hat{T}_1$ decay exponentially, so we find the right hand side of (26) decays exponentially, and so we get similar boundary conditions to the leading order case:

$$\hat{u}_{2y} + N_\infty\hat{u}_2 = 0, \qquad \hat{v}_2 = \hat{v}_{2\infty} - \frac{N_\infty(\gamma-1)\xi}{\sigma}\hat{T}_2 - \frac{\mathrm{i}K}{N_\infty}\hat{u}_2, \qquad \hat{T}_{2y} + \sigma N_\infty\hat{T}_2 = 0 \qquad \text{at } y = Y. \tag{27}$$

The double frequency solution behaves similarly to the leading order acoustics. The branch cut for N_∞ is the same as for η_∞, and we can take the decaying solution and rewrite the equations to ensure only this solution is admitted. However, unlike the leading order case where the boundary condition on $\hat{v}_1$ was matching to the outer solution as $y \to \infty$ through $\hat{v}_{1\infty}$, here the boundary condition on $\hat{v}_2$ is the impedance boundary condition at $y = 0$, since we do not have any freedom to chose Ω and K to match this boundary condition later. The outer solution must still match with $\hat{v}_{1\infty}$, and therefore $\hat{v}_{1\infty}$ provides a boundary condition to the outer solution, calculated below.

The situation is potentially very different for the 'zero' frequency case, however, since necessarily N_∞^2 is always real, and the resulting behaviour depends on the sign of N_∞^2. For downstream decaying modes, $N_\infty^2 < 0$, and both exponentials have purely imaginary argument and oscillate without decaying. In effect, this is because in this case the whole lower-half k-plane is mapped to the branch cut under the transformation $\Omega = \omega - \omega^\star$, $K = k - k^\star$. This means that the $O(\varepsilon^2/\delta^2)$ 'zero' frequency amplification will propagate out of the mean flow boundary layer and into the centre of the duct. For upstream decaying modes, $N_\infty^2 > 0$, and the decaying solution may be taken similarly to the double frequency case. It is worth noting that the impedance boundary condition in the 'zero' frequency case is necessarily $\hat{v}_2 = 0$ at $y = 0$, since an oscillating wall at zero frequency is necessarily rigid.

2. Outer solution in the duct interior

Applying the asymptotic expansion (11) to the governing equations (10) and equating terms of order ε^2, the resulting equations may be rearranged into a Bessel equation forced by the linear outer solution,

$$\begin{aligned}\hat{p}_{O2rr} + \frac{1}{r}\hat{p}_{O2r} + \left((\Omega - MK)^2 - K^2 - \frac{\mathcal{M}^2}{r^2}\right)\hat{p}_{O2} = {} & \frac{(\gamma-1)\xi^2\eta_\infty^2 N_\infty^2}{2}\hat{p}^\star_{O1}\hat{T}_1 - \frac{(\gamma-1)\xi^2 N_\infty^4}{2}\hat{p}^\star_{O1}\hat{T}_{O1} \\ & - \frac{\mathrm{i}K\xi N_\infty^2}{2}\hat{p}^\star_{O1}\hat{u}_{O1} + \frac{\xi N_\infty^2}{2}\left(\frac{\hat{v}_{O1}}{r} + \hat{v}_{O1r}\right)\hat{p}^\star_{O1} + \frac{\xi N_\infty^2}{2}\hat{v}_{O1}\hat{p}^\star_{O1r} - \frac{i\mathcal{M}\xi N_\infty^2}{2r}\hat{w}_{O1}\hat{p}^\star_{O1} \\ & + \frac{\mathrm{i}K}{2}[\xi\eta_\infty^2\hat{p}^\star_{O1}\hat{u}_{O1} - \mathrm{i}k\hat{u}^\star_{O1}\hat{u}_{O1} + \hat{v}^\star_{O1}\hat{u}_{O1r} - \frac{\mathrm{i}m}{r}\hat{w}^\star_{O1}\hat{u}_{O1}] \\ & + \frac{1}{2r}[-\xi\eta_\infty^2\hat{p}^\star_{O1}\hat{v}_{O1} + \mathrm{i}k\hat{u}^\star_{O1}\hat{v}_{O1} - \hat{v}^\star_{O1}\hat{v}_{O1r} + \frac{\mathrm{i}m}{r}\hat{w}^\star_{O1}\hat{v}_{O1} + \frac{1}{r}\hat{w}^\star_{O1}\hat{w}_{O1}] \\ & + \frac{1}{2}[-\xi\eta_\infty^2\hat{p}^\star_{O1}\hat{v}_{O1} + \mathrm{i}k\hat{u}^\star_{O1}\hat{v}_{O1} - \hat{v}^\star_{O1}\hat{v}_{O1r} + \frac{\mathrm{i}m}{r}\hat{w}^\star_{O1}\hat{v}_{O1} + \frac{1}{r}\hat{w}^\star_{O1}\hat{w}_{O1}]_r \\ & + \frac{\mathrm{i}\mathcal{M}}{2r}[-\hat{p}^\star_{O1}\eta_\infty^2\xi\hat{w}_{O1} + \mathrm{i}k\hat{u}^\star_{O1}\hat{w}_{O1} - \hat{v}^\star_{O1}\hat{w}_{O1r} + \frac{\mathrm{i}m}{r}\hat{w}^\star_{O1}\hat{w}_{O1} - \frac{1}{r}\hat{v}^\star_{O1}\hat{w}_{O1}], \end{aligned} \quad (28)$$

where, as before, in the double-frequency case $\Omega = 2\omega$, $K = 2k$, $\mathcal{M} = 2m$ and the $\star$ is ignored, while in the 'zero'-frequency case $\Omega = \omega - \omega^\star$, $K = k - k^\star$, $\mathcal{M} = 0$ and the $\star$ denotes the complex conjugate.

The boundary conditions to be applied to (28) are regularity at $r = 0$, as for the linear case, and matching to the inner solution as $r \to 1$, implying $\hat{p}_{O2}(1) = \hat{p}_2/\delta$ and $\hat{v}_{O2}(1) = \hat{v}_{2\infty}/\delta$. Since these terms are $O(1/\delta)$, so too is $\hat{p}_{O2}$ and consequently the other outer nonlinear variables, and so the forcing on the right hand side of (28), which gives an $O(1)$ effect, is relatively unimportant and is dominated by the $O(1/\delta)$ effect of the inner solution. Here , these terms are nonetheless included, and equation (28) is solved numerically.

Note that for the 'zero' frequency inner solution in the case $N_\infty^2 < 0$, the inner solution does not tend to a constant, and so cannot be matched to this outer solution; this is considered separately in section IV.B.3 below.

3. Outer solution for self-interaction nonlinear components with $N_\infty^2 < 0$

In the case $N_\infty^2 < 0$, the inner solution remains highly oscillatory outside the mean flow boundary layer, and does not match with the outer solution (28). This is because, as the wavelength of the oscillations is short, of $O(\delta)$, the gradients outside the mean flow boundary layer become large and the viscous terms cannot be ignored. By including the viscous terms and rapid oscillation, an asymptotic solution to the outer equations at $O(\varepsilon^2)$ may be found using the method of multiple scales, capable of matching with the inner solution within the mean flow boundary layer. The derivation of this solution is given in appendix A. The result from equation (63) is that, away from the duct centreline $r = 0$,

$$\varepsilon^2\hat{T}_{O2} = \frac{\varepsilon^2}{\delta^2}\frac{\hat{T}_{2\infty}}{\sqrt{r}}\cos\left(\frac{\beta\sigma}{\delta}r - \frac{\pi}{4}\right) + O\left(\frac{\varepsilon^2}{\delta}\right) \quad (29a)$$

$$\varepsilon^2\hat{u}_{O2} = \frac{\varepsilon^2}{\delta^2}\frac{\hat{u}_{2\infty}}{\sqrt{r}}\cos\left(\frac{\beta}{\delta}r - \frac{\pi}{4}\right) + O\left(\frac{\varepsilon^2}{\delta}\right) \quad (29b)$$

$$\varepsilon^2\hat{v}_{O2} = \frac{\varepsilon^2}{\delta}\left[\frac{\mathrm{i}K\hat{u}_{2\infty}}{\beta\sqrt{r}}\sin\left(\frac{\beta}{\delta}r - \frac{\pi}{4}\right) - \frac{\beta\xi(\gamma-1)\hat{T}_{2\infty}}{\sigma\sqrt{r}}\sin\left(\frac{\beta\sigma}{\delta}r - \frac{\pi}{4}\right) + D\frac{J_0'(\Lambda r)}{J_0'(\Lambda)}\right] + O(\varepsilon^2) \quad (29c)$$

$$\varepsilon^2\hat{p}_{O2} = -\frac{\varepsilon^2}{\delta}D\frac{\mathrm{i}(\Omega - MK)}{\Lambda J_0'(\Lambda)}J_0(\Lambda r) + O(\varepsilon^2), \quad (29d)$$

where $\beta^2 = -\mathrm{i}(\Omega - MK)/\xi$, $\Lambda^2 = (\Omega - MK)^2 - K^2$, and the constants $\hat{T}_{2\infty}$, $\hat{u}_{2\infty}$ and D are to be matched to the inner solution within the mean flow boundary layer. At $y = Y \gg 1$, the inner solution is governed by (26). Matching $\hat{u}_2$ and $\hat{T}_2$ at $y = Y \gg 1$ therefore gives two boundary conditions on the inner solution within the boundary layer,

$$\hat{u}_{2y} = -\hat{u}_2\beta\tan\left(\beta y - \frac{\beta}{\delta} + \frac{\pi}{4}\right) \qquad \text{at } y = Y, \quad (30a)$$

$$\hat{T}_{2y} = -\hat{T}_2\beta\sigma\tan\left(\beta\sigma y - \frac{\beta\sigma}{\delta} + \frac{\pi}{4}\right) \qquad \text{at } y = Y, \quad (30b)$$

and sets the two constants $\hat{u}_{2\infty}$ and $\hat{T}_{2\infty}$ in the outer solution,

$$\hat{u}_{2\infty} = \frac{1}{\mathrm{i}\beta}\mathrm{e}^{\mathrm{i}\beta y - \mathrm{i}\beta/\delta + \mathrm{i}\frac{\pi}{4}}(\mathrm{i}\beta\hat{u}_2 - \hat{u}_{2y}) \qquad \text{at } y = Y, \tag{31}$$

$$\hat{T}_{2\infty} = \frac{1}{\mathrm{i}\beta\sigma}\mathrm{e}^{\mathrm{i}\beta\sigma y - \mathrm{i}\beta\sigma/\delta + \mathrm{i}\frac{\pi}{4}}(\mathrm{i}\beta\sigma\hat{T}_2 - \hat{T}_{2y}) \qquad \text{at } y = Y. \tag{32}$$

Similarly, matching $\hat{v}_2$ and $\hat{v}_{O2}$ at $y = Y \gg 1$ leads to

$$D = \hat{v}_2 + \frac{\mathrm{i}K\hat{u}_{2\infty}}{\beta}\sin\left(\beta y - \frac{\beta}{\delta} + \frac{\pi}{4}\right) - \frac{\beta\xi(\gamma-1)\hat{T}_{2\infty}}{\sigma}\sin\left(\beta\sigma y - \frac{\beta\sigma}{\delta} + \frac{\pi}{4}\right) \qquad \text{at } y = Y. \tag{33}$$

Since the contribution from the inner solutions are $O(\varepsilon^2/\delta^2)$ and do not decay, the constants $\tilde{u}_{2\infty}$ and $\tilde{T}_{2\infty}$, once matched, are both $O(1)$. These outer solutions therefore contribute an $O(\varepsilon^2/\delta^2)$ amplified acoustic streaming, stronger than the $O(\varepsilon^2)$ acoustic streaming that would be expected, that is caused by the viscous mean flow boundary layer over the acoustic lining. An example of this behaviour is given later in figure 7.

Also from equation (63) in appendix A, the leading order behaviour of $\hat{u}_{O2}$ and $\hat{T}_{O2}$ near the duct centreline $r = 0$ is given as

$$\varepsilon^2\hat{T}_{O2} = \frac{\varepsilon^2}{\delta^{5/2}}\hat{T}_{2\infty}\sqrt{\frac{\beta\sigma\pi}{2}}J_0\left(\frac{\beta\sigma}{\delta}r\right) + O\left(\frac{\varepsilon^2}{\delta}\right), \tag{34a}$$

$$\varepsilon^2\hat{u}_{O2} = \frac{\varepsilon^2}{\delta^{5/2}}\hat{u}_{2\infty}\sqrt{\frac{\beta\pi}{2}}J_0\left(\frac{\beta}{\delta}r\right) + O\left(\frac{\varepsilon^2}{\delta}\right), \tag{34b}$$

showing that near the centreline $r = 0$ the oscillatory solutions grow from $O(\varepsilon^2/\delta^2)$ to $O(\varepsilon^2/\delta^{5/2})$. This will also be seen later in figure 7.

4. Interaction of multiple modes

We might also consider the nonlinear effect due to two different frequency leading order modes interacting. We now take the leading order acoustics as a superposition of two waves,

$$\tilde{u}_1 = \mathrm{Re}\left(\hat{u}_{1a}e^{\mathrm{i}(\omega_a t - k_a x - m_a\theta)}\right) + \mathrm{Re}\left(\hat{u}_{1b}e^{\mathrm{i}(\omega_b t - k_b x - m_b\theta)}\right), \tag{35}$$

We finally obtain two pairs of nonlinear self-interaction Fourier components, as described above, as well as two cross-interaction components. These cross-interactions components will have the forms

$$\tilde{u}_{2+} = \mathrm{Re}\big(\hat{u}_{2+}e^{\mathrm{i}[(\omega_a+\omega_b)t-(k_a+k_b)x-(m_a+m_b)\theta]}\big), \qquad \tilde{u}_{2-} = \mathrm{Re}\big(\hat{u}_{2-}e^{\mathrm{i}[(\omega_a-\omega_b^\star)t-(k_a-k_b^\star)x-(m_a-m_b)\theta]}\big). \tag{36}$$

The system of equations we now have to solve are:

$$\mathcal{L}(\hat{u}_{2+}, \hat{v}_{2+}, \hat{T}_{2+}; \Omega, K) = Q(\hat{u}_{1a}, \hat{v}_{1a}, \hat{T}_{1a}; \hat{u}_{1b}, \hat{v}_{1b}, \hat{T}_{1b}; \omega_a, k_a) + Q(\hat{u}_{1b}, \hat{v}_{1b}, \hat{T}_{1b}; \hat{u}_{1a}, \hat{v}_{1a}, \hat{T}_{1a}; \omega_b, k_b) \tag{37}$$

with Q from (25), $\Omega = \omega_a + \omega_b$ and $K = k_a + k_b$, and

$$\mathcal{L}(\hat{u}_{2-}, \hat{v}_{2-}, \hat{T}_{2-}; \Omega, K) = Q(\hat{u}_{1a}, \hat{v}_{1a}, \hat{T}_{1a}; \hat{u}_{1b}^\star, \hat{v}_{1b}^\star, \hat{T}_{1b}^\star; \omega_a, k_a) + Q(\hat{u}_{1b}^\star, \hat{v}_{1b}^\star, \hat{T}_{1b}^\star; \hat{u}_{1a}, \hat{v}_{1a}, \hat{T}_{1a}; -\omega_b^\star, -k_b^\star) \tag{38}$$

with $\Omega = \omega_a - \omega_b^\star$ and $K = k_a - k_b^\star$.

The magnitude of the matching outer solution depends on N_∞^2 in the same way as the self-interaction solutions. For N_∞^2 real and negative the outer solution is $O(\varepsilon^2/\delta^2)$, and for all other values of N_∞^2 it is $O(\varepsilon^2/\delta)$. However, for N_∞^2 to be real and negative a rather particular choice of ω_a, ω_b, k_a and k_b is needed, and the usual case will be of $O(\varepsilon^2/\delta)$ and therefore the amplification is expected to remain contained within the mean flow boundary layer for most nonlinear wave interactions.

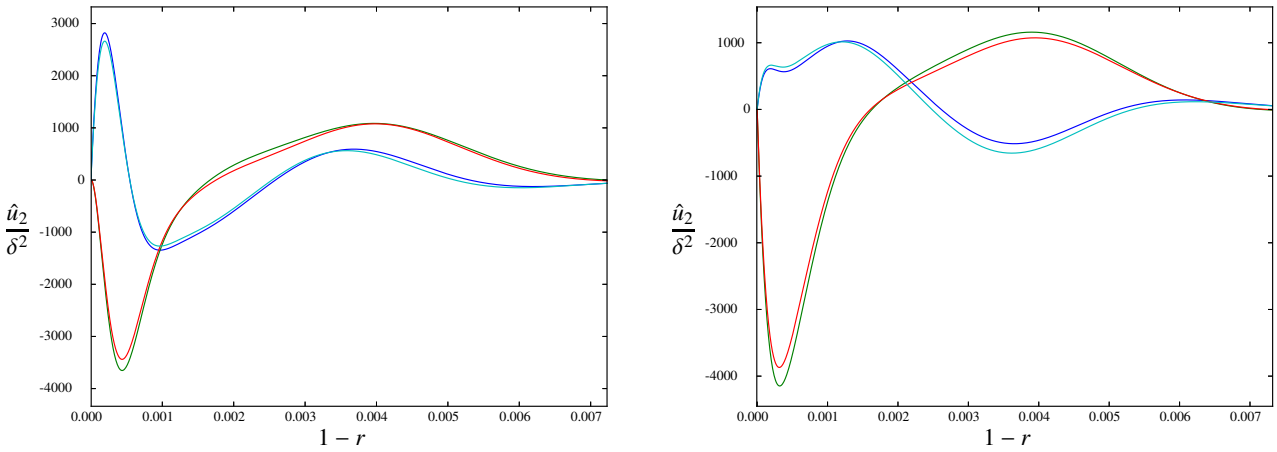

Fig. 4 Inner solutions of $\hat{u}_{2+}/\delta^2$ (left) and $\hat{u}_{2-}/\delta^2$ (right) for $\omega_a = 5$, $k_a = 10$, $m_a = 10$, $\omega_b = 31 + 5i$, $k_b = 12$, $m_b = 12$ for asymptotics (real part dark blue, imaginary part green) compared to the WNLNSE (real part light blue, imaginary part red), with $\delta = 10^{-3}$, $M = 0.7$, Pr $= 0.7$ and $\xi = 0.8$, giving Re $= 1.25 \times 10^6$.

V. Numerical Results

In what follows, a number of examples are computed and described. The parameters for these examples are chosen to illustrate the range of different behaviours achievable. The examples are not intended to represent realistic choices of parameters for any particular practical application. In particular, the values of ω and k chosen would only correspond to modes if the impedance at the duct wall at $r = 1$ takes the particular value $Z = \hat{p}_1(1)/\hat{v}_1(1)$.

While asymptotic approximate solutions to equations (19,25,37) are possible [see, e.g. 2, 17], here these equations are solved numerically using 4th order finite differences. The resulting $3N \times 3N$ banded matrix system of equations is solved using the LAPACK_ZGBSV routine. To solve for the first order nonlinear inner, the same matrix is used, now forced by terms nonlinear in the leading order quantities. The system of equations is solved from $y = 0$ to $y = Y$, where Y is chosen large enough so that the mean flow terms are approximately their uniform mean flow values, and the extrapolation condition (20) is used as the boundary condition.

By way of comparison, we also produce numerical solutions to the Weakly Non-Linear Navier Stokes Equations (WNLNSE), formed by expanding the full Navier Stokes equations to leading and first order in ε, without any of the asymptotic assumptions in δ and the matching needed above. The WNLNSE are solved numerically using a 4th order finite difference scheme for the $O(\varepsilon)$ and $O(\varepsilon^2)$ equations thus obtained. In this case we get a $5N \times 5N$ banded matrix equation that is homogeneous in the leading order case and forced by leading order terms in the first order case. In order to accurately resolve the details in the mean flow boundary layer while still solving across the whole duct, the numerical points are equally spaced in a stretched coordinates $r_s = \tanh(Sr)/\tanh(S)$, where S is the stretching factor. This concentrates the grid points about $r = 1$ so that the rapid variations there due to the thin mean flow boundary layer are properly resolved. For the results below a stretching factor of $S = 2.0$ is used. Before solving, the matrix is balanced so that the largest value in each row is 1; this ensures that the solution remains stable near the origin, where terms involving $1/r$ can become large.

The boundary conditions at the origin for the WNLNSE are found by assuming all quantities have a regular series expansion near the origin and matching powers of $1/r$. This eliminates the possibility of any non-regular terms in the acoustic quantities and gives boundary conditions that are consistent with the expected Bessel function solutions.

Presented below in figures 4–7 are plots of the weakly nonlinear axial velocity, scaled such that the contribution to the overall axial velocity is ε^2 times what is plotted; this scaling means that the results are independent of the actual amplitude ε chosen. From the outer scaling (11) this means plotting $\hat{u}_{O2}$ as the solution outside the mean flow boundary layer, while from the inner scaling (15b) this means plotting $\hat{u}_2/\delta^2$ as the solution inside the mean flow boundary layer.

Figure 4 shows plots of the axial velocity for both types of cross-interaction solutions. The asymptotic solution can be seen to be in good agreement with the WNLNSE, calculated without assumptions about thin mean flow boundary layers and matching. Note that these solutions are normalized so that $\hat{p}_1 = 1$ at the wall.

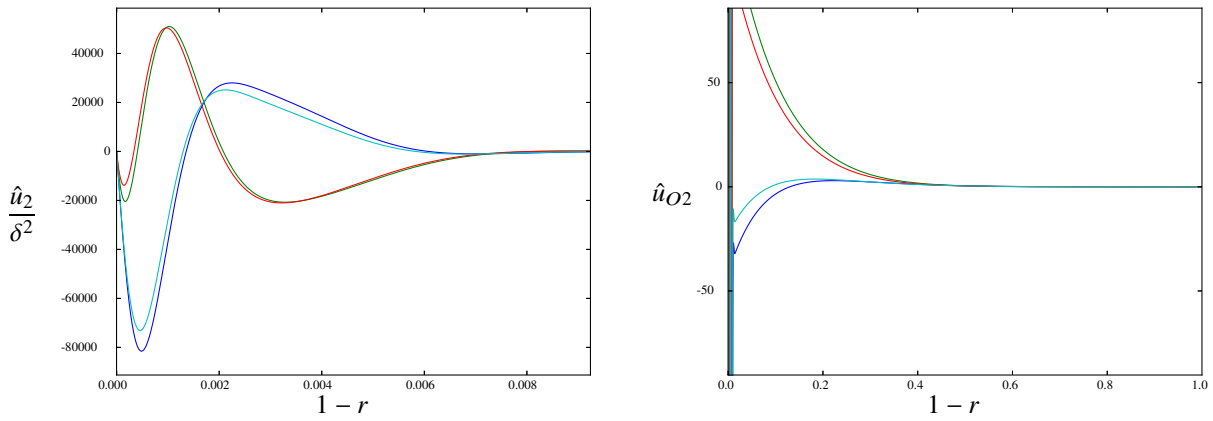

Fig. 5 Inner ($\hat{u}_2/\delta^2$, left) and outer ($\hat{u}_{O2}$, right) profiles of the double frequency solution, comparing the asymptotics (real part dark blue, imaginary part green) to the first term from the WNLNSE (real part light blue, imaginary part red). Parameters are $\omega = 5$, $k = 5 + \mathbf{i}$, $m = 2$, Pr $= 0.7$, $M = 0.7$, $\delta = 10^{-3}$, and $\xi = 0.8$, giving $\mathrm{Re} = 1.25 \times 10^6$**.**

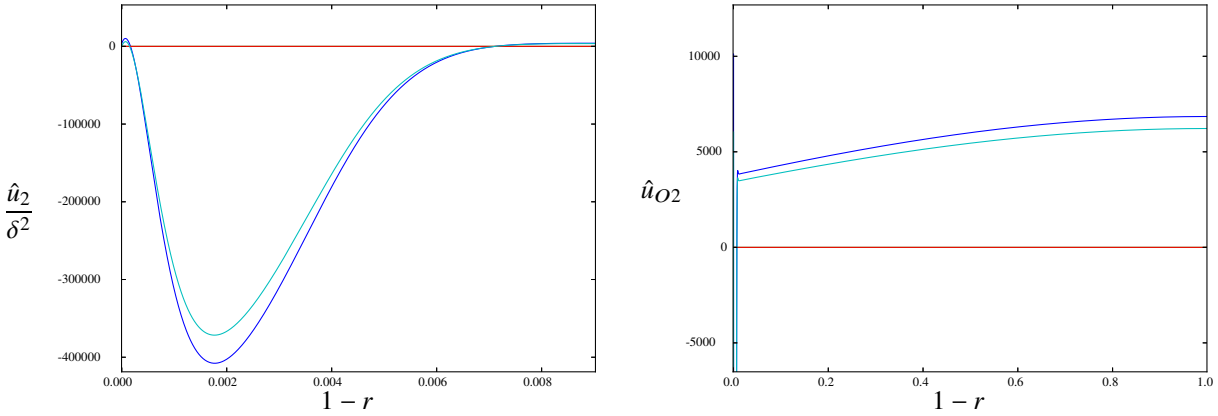

Fig. 6 Inner ($\hat{u}_2/\delta^2$, left) and outer ($\hat{u}_{O2}$, right) profiles of the 'zero' frequency nonlinear component for $\omega = 5$, $k = 5 + \mathbf{i}$ and $m = 2$ for asymptotics (real part dark blue, imaginary part green) compared to the first term from the WNLNSE (real part light blue, imaginary part red). Other parameters are $M = 0.7$, $\delta = 10^{-3}$, Pr $= 0.7$ and $\xi = 0.8$, corresponding to $\mathrm{Re} = 1.25 \times 10^6$**.**

A typical profile of the double-frequency nonlinear solution is given in figure 5. The nonlinear asymptotic solution is shown to be in good agreement with be first term from the WNLNSE, giving confidence in the asymptotic method applied. Moreover, both solutions are localized within the mean flow boundary layer ($\delta = 10^{-3}$ in this case), confirming the prediction that the $O(1/\delta)$ amplification within the mean flow boundary layer [2] does indeed trigger significantly more nonlinearity than would otherwise have been expected, but that, for the double frequency solution, it does not bleed out into the rest of the duct.

The comparable 'zero' frequency nonlinear solution, for the case upstream decaying case $N_\infty^2 > 0$, is plotted in figure 6. This shows a similar trend to figure 5, in that the predicted $O(1/\delta)$ amplification within the mean flow boundary layer is seen, but does not bleed out into the rest of the duct; the acoustic streaming in the centre of the duct remains the classical magnitude of $O(\varepsilon^2\delta^0)$. Figure 5 could be compared to Rayleigh streaming [e.g. 25], since there is acoustic streaming (motion at zero frequency) in one direction within the mean flow boundary layer and in the other direction outside the mean flow boundary layer. However, this differs from classical Rayleigh streaming in a number of ways, including that the boundary layer concerned is the mean flow boundary layer and not the acoustic boundary layer, that the effect in figure 5 is inviscid while Rayleigh streaming is viscous, and that the effect in figure 5 is axially uniform instead of consisting axially of cells as it would with Rayleigh streaming.

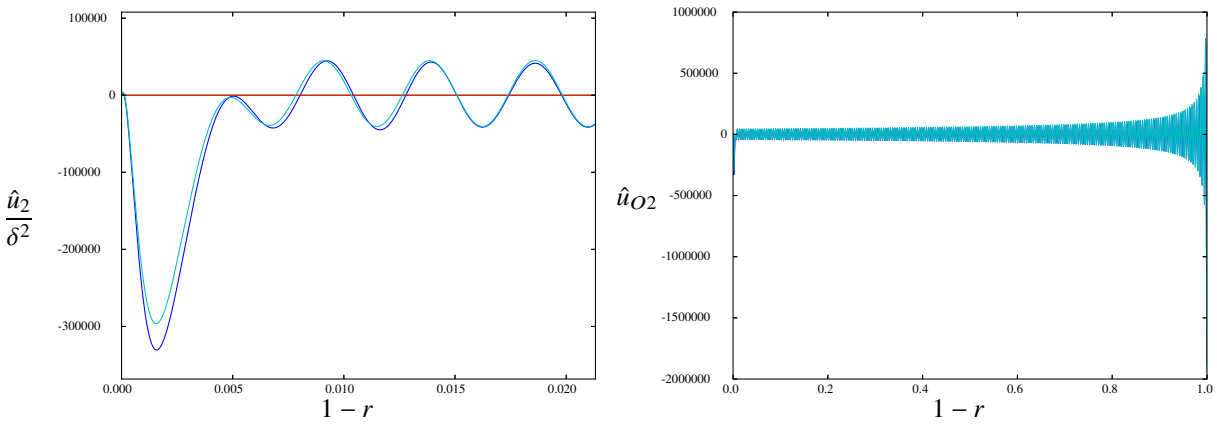

Fig. 7 Inner ($\hat{u}_2/\delta^2$, left) and outer ($\hat{u}_{O2}$, right) of the 'zero' frequency nonlinear component for $\omega = 5$, $k = 5 - \mathbf{i}$ and $m = 2$ for asymptotics (real part dark blue, imaginary part green) compared to the first term from the WNLNSE (real part light blue, imaginary part red). Other parameters are $M = 0.7$, $\delta = 10^{-3}$, Pr $= 0.7$ and $\xi = 0.8$, giving to $\mathrm{Re} = 1.25 \times 10^6$.

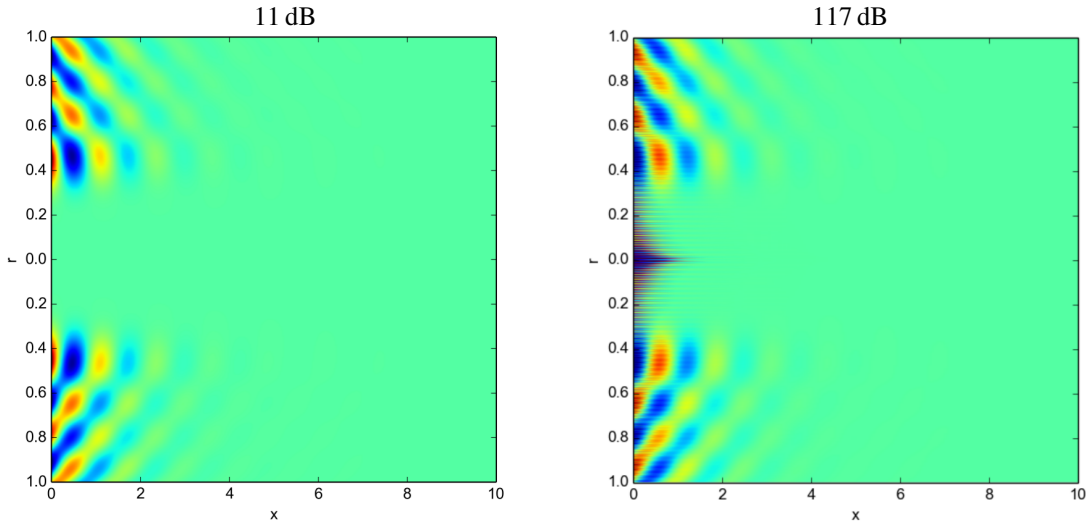

Fig. 8 Plot of snapshots of the total perturbation for $k = 5 - i$, $\omega = 31$, $m = 10$ and $\delta = 10^{-3}$ for different initial amplitudes. The amplitudes are: $\varepsilon = 5 \times 10^{-10}$, giving 11 dB (left); and $\varepsilon = 10^{-4}$, giving 117 dB (right).

In contrast, however, figure 7 shows the profiles in the case of a downstream decaying mode, for which $N_\infty^2 < 0$. The solution is seen to oscillate rapidly in r with the predicted wavelength of order $O(\delta)$ from (29). This amplified rapid oscillation does not decay away from the mean flow boundary layer and is present throughout the duct, with an amplitude of $O(\varepsilon^2/\delta^2)$, growing to $O(\varepsilon^2/\delta^{5/2})$ towards $r = 0$ as predicted in (34). This shows that, in this case, the amplification within the mean flow boundary layer by a factor of $1/\delta$ previously predicted [2] does indeed lead to significant nonlinearity beyond what would have been expected within the duct, and that this nonlinearity is not in this case confined to within the mean flow boundary layer but bleeds out into the rest of the duct.

Figure 8 shows the total sum of these effects, by plotting the overall perturbation to the streamwise velocity $\tilde{u}$ at different acoustic amplitudes. Figure 8 picks a single linear mode $\varepsilon\tilde{u}_1$ introduced on the left of the plots at $x = 0$ with the given amplitudes, and plots the sum of this mode and its induced double-frequency and 'zero'-frequency nonlinear contributions from $\tilde{u}_2$. The effect of the nonlinear streaming is easily seen by the hairy appearance of the louder plot, although this nonlinear perturbation decays faster in the x direction than the damped acoustics, since the axial wavenumber has twice the decay rate of the linear acoustics.

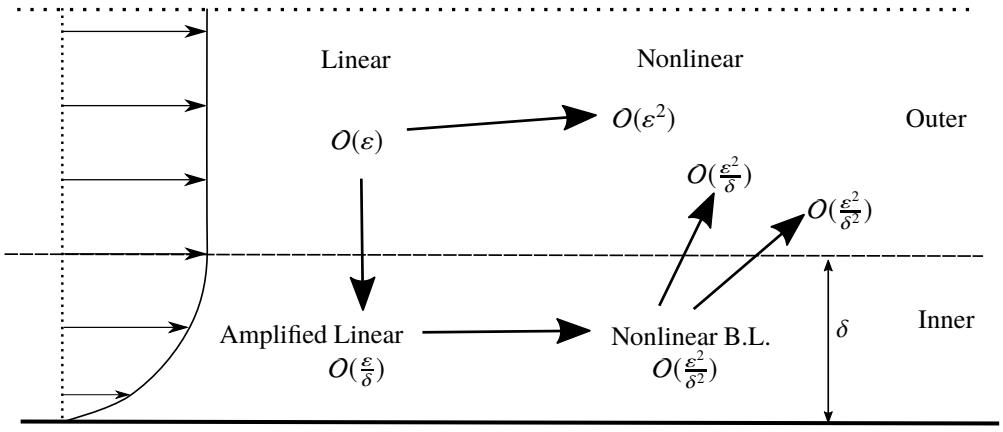

Fig. 9 Diagram of the routes by which the linear amplification within the boundary layer and nonlinear interactions within the boundary layer lead to larger than expected nonlinear acoustics outside the boundary layer.

VI. Conclusion

In this paper, we have investigated how the previously predicted [2] amplification by a factor of $1/\delta$ of acoustics within a thin visco-thermal mean flow boundary layer of thickness δ over an acoustic lining leads to nonlinear effects becoming apparent at lower sound amplitudes than might have otherwise been expected. It is emphasized that the nonlinearity presented here is nonlinearity within the mean flow boundary layer, and is separate to the nonlinear behaviour of the actual boundary, such as the nonlinear behaviour of Helmholtz resonators near resonance [4]. A schematic diagram of the routes leading to this amplification is given in figure 9. The mechanism is that sound of amplitude ε enters the mean flow boundary layer of thickness δ and is amplified to order ε/δ. Nonlinear interactions then result in new acoustics with an amplitude of order ε^2/δ^2. These new acoustics have either double the frequency of the incoming sound, or 'zero' times the frequency, the latter corresponding to acoustic streaming. The double frequency amplified sound within the boundary layer leads to double frequency sound in the rest of the duct of order ε^2/δ, a factor of $1/\delta$ larger than would have been expected from nonlinear interactions within the duct itself. By contrast, for downstream decaying sound the 'zero' frequency nonlinear component bleed into the rest of the duct and show an order ε^2/δ^2 amplitude throughout the duct and a rapid radial oscillation with a wavelength of order δ. This amplification is a factor of $1/\delta^2$ times the magnitude that would be created by ordinary nonlinear interactions within the duct itself.

This is an unexpected result as one would not expect such highly oscillatory solutions in the centre of the duct. However this behaviour is present in both our asymptotic solution and in the numerical results from the weakly nonlinear Navier Stokes equations (WNLNSE). Since these solutions have only been identified mathematically, it would be interesting to look for their signature in existing experimental results, such as those of Aurégan and Leroux [3], for example. It is also possible that this behaviour is a consequence of one of our assumptions. It would therefore be interesting in future to investigate the effect of weakening some of our assumptions, in particular that of uniform mean flow, as in real aircraft engines we would expect to have a developing mean flow boundary layer profile.

Also derived here are equations governing the nonlinear interactions of two modes of differing frequencies. As for the self-interacting case, nonlinearity becomes important at lower amplitudes than expected due to the $1/\delta$ amplification within the mean flow boundary layer. Such interactions may well be important when two well-damped high azimuthal order spinning modes (for example, corresponding to the number of rotor and stator blades respectively) interact to produce a poorly-damped low azimuthal order nonlinear solution. Another such case might be a pair of helical modes $(\omega, k, \pm m)$ interacting, giving a "zero-frequency" component with an azimuthal wavenumber $2m$, although in aeroacoustics applications such symmetry would usually be broken by the direction of rotation of the rotor blades.

So far, this analysis has not been applied to investigate nonlinearity within surface modes [10, 26]. Since surface modes are localized close to the boundary, and since one of them might be an instability which might lead to large amplitudes, investigating the impact of nonlinearity on such modes in combination with the $1/\delta$ amplification would prove interesting. For example, it may be that the nonlinearity enhances certain surface modes and restrains others.

The analysis presented here has assumed a thin mean flow boundary layer of width δ, and a small acoustic perturbation of amplitude ε, with $\varepsilon \ll \delta \ll 1$. In practice this is expected to be applicable to aircraft engines up to

about 150 dB, depending on the boundary layer thickness, and at such amplitudes nonlinear effects are expected to become important everywhere and not just confined to the mean flow boundary layers. While the use of the asymptotics simplifies the governing equations, numerical solutions are still needed. In the linear case, other additional methods have been used [2, 16, 17] to derive approximate solutions and an effective impedance Z_{eff} that accounts for the behaviour within the mean flow boundary layer without having to numerically solve differential equations, and such techniques may well be applicable here.

Finally, the analysis presented here is valid for arbitrary parallel mean flow boundary layer profiles, and not just the Blasius boundary layer profile used for the numerical examples here, provided that the mean flow boundary layer is parallel and not axially developing. The authors hope to study weak nonlinearity in a slowly developing mean flow boundary layer in a future publication.

Funding Sources

ODP is grateful for funding from a Trinity College Graduate Studentship from Trinity College, Cambridge, UK.
EJB is grateful for funding from the Royal Society as a University Research Fellow (grant number UF150695).

A. Outer Solution for Oscillating Nonlinear Self-interaction

This appendix gives the derivation of the nonlinear self-interaction outer solutions in the oscillatory case $N_\infty^2 < 0$. From (15) we know that the weakly-nonlinear solution within the boundary layer contributes to both $\tilde{u}$ and $\tilde{T}$ at order $O(\varepsilon^2/\delta^2)$, while contributing to $\tilde{v}$, $\tilde{p}$ and $\tilde{w}$ only at $O(\varepsilon^2/\delta)$. In the case we consider here, $N_\infty^2 < 0$, equation (26) shows that the weakly nonlinear solutions $\hat{u}_2$, $\hat{T}_2$ and $\hat{v}_2$ do not decay away from the mean flow boundary layer, but instead rapidly oscillate on the length scale $y = O(1)$, $r = O(1/\delta)$; because of this, they cannot match to the outer solution given in (28), since this outer solution was derived from governing equations (10) which neglect such rapid oscillations. Note that the weakly-nonlinear component of pressure, $\hat{p}_2$, is also $O(\varepsilon^2/\delta)$, like $\hat{v}_2$, but unlike $\hat{v}_2$ it is constant over the boundary layer and so is not rapidly oscillating. Our task, therefore, is to find a new outer solution which matches to these highly-oscillatory inner solutions. To do this we allow for rapid oscillations in the outer solution by using the Method of Multiple Scales, introducing a fast scale y and a slow scale R such that $r = R - \delta y$, and hence $\partial/\partial r = \partial/\partial R - \delta^{-1}\partial/\partial y$. Evaluating this solution along $R = r$ and $y = -r/\delta$ gives the Multiple Scales solution in the original variable r. We then consider the full governing equations (1) outside the mean flow boundary layer, so that $T_0 = 1/(\gamma - 1)$, $p_0 = 1/\gamma$, and $\rho_0 = 1$, but retain the viscous terms that were dropped when deriving (10). We then expand using the asymptotic expansion (11), but in order to match with the inner solution we further expand the $O(\varepsilon^2)$ weakly-nonlinear terms in powers of δ,

$$\tilde{T}_{O2} = \text{Re}\Big(\frac{1}{\delta^2}\big[\hat{T}_{\Theta 0} + \delta\hat{T}_{\Theta 1} + \delta^2\hat{T}_{\Theta 2} + O(\delta^3)\big]\exp\big\{\text{i}\Omega t - \text{i}Kx\big\}\Big), \tag{39a}$$

$$\tilde{u}_{O2} = \text{Re}\Big(\frac{1}{\delta^2}\big[\hat{u}_{\Theta 0} + \delta\hat{u}_{\Theta 1} + \delta^2\hat{u}_{\Theta 2} + O(\delta^3)\big]\exp\big\{\text{i}\Omega t - \text{i}Kx\big\}\Big), \tag{39b}$$

$$\tilde{v}_{O2} = \text{Re}\Big(\frac{1}{\delta}\big[\hat{v}_{\Theta 0} + \delta\hat{v}_{\Theta 1} + \delta^2\hat{v}_{\Theta 2} + O(\delta^3)\big]\exp\big\{\text{i}\Omega t - \text{i}Kx\big\}\Big), \tag{39c}$$

$$\tilde{w}_{O2} = \text{Re}\Big(\frac{1}{\delta}\big[\hat{w}_{\Theta 0} + \delta\hat{w}_{\Theta 1} + \delta^2\hat{w}_{\Theta 2} + O(\delta^3)\big]\exp\big\{\text{i}\Omega t - \text{i}Kx\big\}\Big), \tag{39d}$$

$$\tilde{p}_{O2} = \text{Re}\Big(\frac{1}{\delta}\big[\hat{p}_{\Theta 0} + \delta\hat{p}_{\Theta 1} + \delta^2\hat{p}_{\Theta 2} + O(\delta^3)\big]\exp\big\{\text{i}\Omega t - \text{i}Kx\big\}\Big), \tag{39e}$$

where it is emphasized that $\tilde{T}_{O2}$ and $\tilde{u}_{O2}$ are one order of magnitude in δ larger than the other variables. In what follows, the shorthand $\hat{T}_\Theta = \hat{T}_{\Theta 0} + \delta\hat{T}_{\Theta 1} + \delta^2\hat{T}_{\Theta 2} + \cdots$ will be used, and similarly for the other variables. At $O(\varepsilon^2)$ this leads to the following equations

$$\delta^{-2}\big[-\text{i}(\Omega - MK)(\gamma-1)\hat{T}_\Theta - \text{i}K\hat{u}_\Theta - \hat{v}_{\Theta y}\big] + \delta^{-1}\big[\text{i}(\Omega - MK)\gamma\hat{p}_\Theta + \tfrac{1}{R}(R\hat{v}_\Theta)_R\big] = P_{\text{RHS}} + O(\delta), \tag{40a}$$

$$\begin{aligned}\delta^{-2}\big[\text{i}(\Omega - MK)\hat{u}_\Theta - \xi\hat{u}_{\Theta yy}\big] + \delta^{-1}\big[2\xi\hat{u}_{\Theta Ry} + \tfrac{1}{R}\xi\hat{u}_{\Theta y} - \text{i}K\hat{p}_\Theta\big]\\ + \xi(2+\lambda)K^2\hat{u}_\Theta - \text{i}K\xi(1+\lambda)\hat{v}_{\Theta y} - \tfrac{1}{R}\xi\big(r\hat{u}_{\Theta R}\big)_R = U_{\text{RHS}} + O(\delta),\end{aligned} \tag{40b}$$

$$\begin{aligned}-\delta^{-2}\hat{p}_{\Theta y} + \delta^{-1}\big[\text{i}(\Omega - MK)\hat{v}_\Theta + \hat{p}_{\Theta R} - \xi(2+\lambda)\hat{v}_{\Theta yy} - \text{i}K\xi(1+\lambda)\hat{u}_{\Theta y}\big]\\ + 2(2+\lambda)\xi\hat{v}_{\Theta Ry} + \tfrac{1}{R}(2+\lambda)\xi\hat{v}_{\Theta y} + \text{i}K(1+\lambda)\xi\hat{u}_{\Theta R} = V_{\text{RHS}} + O(\delta),\end{aligned} \tag{40c}$$

$$\delta^{-1}\left[\mathrm{i}(\Omega - MK)\hat{w}_\Theta - \xi\hat{w}_{\Theta yy}\right] + 2\xi\hat{w}_{\Theta Ry} + \tfrac{1}{R}\xi\hat{w}_{\Theta y} = W_{\mathrm{RHS}} + O(\delta), \tag{40d}$$

$$\begin{aligned}\delta^{-2}\left[\mathrm{i}(\Omega - MK)\hat{T}_\Theta - \frac{\xi}{\sigma^2}\hat{T}_{\Theta yy}\right] + \delta^{-1}\Big[- \mathrm{i}(\Omega - MK)\hat{p}_\Theta + 2\frac{\xi}{\sigma^2}\hat{T}_{\Theta Ry} + \frac{\xi}{R\sigma^2}\hat{T}_{\Theta y}\Big] \\ - \frac{\xi}{\sigma^2}\left[\hat{T}_{\Theta RR} + \tfrac{1}{R}\hat{T}_{\Theta R} - K^2\hat{T}_\Theta\right] = T_{\mathrm{RHS}} + O(\delta)\end{aligned} \tag{40e}$$

where $\sigma^2 = \mathrm{Pr}$ is the Prandtl number, $\lambda = (\mu^{\mathrm{B}}/\mu - 2/3)$, and we have used that $\hat{\rho}_\Theta = -(\gamma-1)\hat{T}_\Theta + \delta\gamma\hat{p}_\Theta - \delta^2\frac{(\gamma-1)}{2}\hat{T}_{O1}\hat{\rho}^\star_{O1}$ (from equations 1e, 22 and 39). The right hand side terms are the forcing terms that arise from terms quadratic in the linear acoustics. They are given by:

$$P_{\mathrm{RHS}} = \frac{1}{2}\left(N_\infty^2\xi(\gamma-1)\hat{p}^\star_{O1}\hat{p}_{O1} + \mathrm{i}K\hat{p}^\star_{O1}\hat{u}_{O1} - \tfrac{1}{R}\big(R\hat{p}^\star_{O1}\hat{v}_{O1}\big)_R\right) \tag{41a}$$

$$U_{\mathrm{RHS}} = \frac{1}{2}\left(-\eta_\infty^2\xi\hat{u}_{O1}\hat{p}^\star_{O1} + \mathrm{i}k\hat{u}^\star_{O1}\hat{u}_{O1} - \hat{v}^\star_{O1}\hat{u}_{O1R} + \frac{\mathrm{i}m}{R}\hat{w}^\star_{O1}\hat{u}_{O1}\right) \tag{41b}$$

$$V_{\mathrm{RHS}} = \frac{1}{2}\left(-\eta_\infty^2\xi\hat{v}_{O1}\hat{p}^\star_{O1} + \mathrm{i}k\hat{u}^\star_{O1}\hat{v}_{O1} - \hat{v}^\star_{O1}\hat{v}_{O1R} + \frac{\mathrm{i}m}{R}\hat{w}^\star_{O1}\hat{v}_{O1} + \tfrac{1}{R}\hat{w}^\star_{O1}\hat{w}_{O1}\right) \tag{41c}$$

$$W_{\mathrm{RHS}} = \frac{1}{2}\left(-\eta_\infty^2\xi\hat{w}_{O1}\hat{p}^\star_{O1} + \mathrm{i}k\hat{u}^\star_{O1}\hat{w}_{O1} - \hat{v}^\star_{O1}\hat{w}_{O1R} + \frac{\mathrm{i}m}{R}\hat{w}^\star_{O1}\hat{w}_{O1} - \tfrac{1}{R}\hat{v}^\star_{O1}\hat{w}_{O1}\right) \tag{41d}$$

$$T_{\mathrm{RHS}} = \frac{1}{2}\left(-\eta_\infty^2\xi\hat{p}_{O1}\hat{p}^\star_{O1}\right) \tag{41e}$$

where we have used that $\hat{T}_{O1} = \hat{\rho}_{O1} = \hat{p}_{O1}$ (from equation 18).

First of all, expanding $\hat{p}_\Theta$ and equating powers of δ in the radial the radial momentum equation (40c) gives

$$O(\delta^{-2}): \qquad \hat{p}_{\Theta 0y} = 0, \tag{42a}$$

$$O(\delta^{-1}): \qquad \hat{p}_{\Theta 1y} = \hat{p}_{\Theta 0R} + \xi N_\infty^2\hat{v}_{\Theta 0} - \xi(2+\lambda)\hat{v}_{\Theta 0yy} - \mathrm{i}K\xi(1+\lambda)\hat{u}_{\Theta 0y}, \tag{42b}$$

$$\begin{aligned}O(1): \qquad \hat{p}_{\Theta 2y} = \hat{p}_{\Theta 1R} + \xi N_\infty^2\hat{v}_{\Theta 1} - \xi(2+\lambda)\hat{v}_{\Theta 1yy} - \mathrm{i}K\xi(1+\lambda)\hat{u}_{\Theta 1y} \\ + 2(2+\lambda)\xi\hat{v}_{\Theta 0Ry} + \tfrac{1}{R}(2+\lambda)\xi\hat{v}_{\Theta 0y} + \mathrm{i}K(1+\lambda)\xi\hat{u}_{\Theta 0R} - V_{\mathrm{RHS}}.\end{aligned} \tag{42c}$$

The $O(\delta^{-2})$ equation implies that $\hat{p}_\Theta = \bar{p}(R)$ is only a function of the slow variable R and is not rapidly oscillating, which agrees with the solution within the mean flow boundary layer. We will return to the high order equations below.

Next, equating powers of δ in the streamwise momentum equation (40b) gives

$$O(\delta^{-2}): \qquad N_\infty^2\hat{u}_{\Theta 0} - \hat{u}_{\Theta 0yy} = 0 \tag{43a}$$

$$O(\delta^{-1}): \qquad N_\infty^2\hat{u}_{\Theta 1} - \hat{u}_{\Theta 1yy} = -2\hat{u}_{\Theta 0yR} - \frac{\hat{u}_{\Theta 0y}}{R} + \frac{\mathrm{i}K}{\xi}\hat{p}_{\Theta 0} \tag{43b}$$

$$\begin{aligned}O(1): \qquad N_\infty^2\hat{u}_{\Theta 2} - \hat{u}_{\Theta 2yy} = -2\hat{u}_{\Theta 1Ry} - \frac{\hat{u}_{\Theta 1y}}{R} + \frac{\mathrm{i}K}{\xi}\hat{p}_{\Theta 1} \\ - (2+\lambda)K^2\hat{u}_{\Theta 0} + \mathrm{i}K(1+\lambda)\hat{v}_{\Theta 0y} + \hat{u}_{\Theta 0RR} + \tfrac{1}{R}\hat{u}_{\Theta 0R} + U_{RHS}\end{aligned} \tag{43c}$$

We may solve the leading order $O(\delta^{-2})$ equation for $\hat{u}_{\Theta 0}$, giving

$$\hat{u}_{\Theta 0} = A_1(R)e^{\mathrm{i}\beta y} + A_2(R)e^{-\mathrm{i}\beta y} \qquad \text{where} \qquad \beta^2 = -N_\infty^2 \tag{44}$$

Substituting this into the next order equation (43b), we find

$$\hat{u}_{\Theta 1yy} - N_\infty^2\hat{u}_{\Theta 1} = \mathrm{i}\beta e^{\mathrm{i}\beta y}\left(2A_{1R} + \frac{A_1}{R}\right) - \mathrm{i}\beta e^{-\mathrm{i}\beta y}\left(2A_{2R} + \frac{A_2}{R}\right) + \frac{\mathrm{i}K}{\xi}\hat{p}_{\Theta 0}(R). \tag{45}$$

To avoid a secular term that grows rapidly on the short lengthscale y, we require that both exponential terms on the right hand side vanish. This implies that $2A_{1R} + A_1/R = 0$, meaning that $A_1(R) = a_1R^{-1/2}$ for some constant a_1, and similarly for A_2. Hence,

$$\hat{u}_{\Theta 0} = R^{-1/2}\big(a_1e^{\mathrm{i}\beta y} + a_2e^{-\mathrm{i}\beta y}\big). \tag{46}$$

Evaluating this solution along $R = r$ and $y = -r/\delta$ gives the Multiple Scales solution. However, this solution is generally singular at $r = 0$ due to the $1/R$ terms, and so enforcing regularity at $r = 0$ provides one of the two constants on a_1 and a_2. To formulate this constraint, we need to solve for $\tilde{u}_{O2}(r)$ about $r = 0$ where the $1/r$ terms become large. To do this we set $r = \delta q$ and expand the governing equations (1) to leading order in δ; this may also be accomplished by setting $R = \delta q$ in (40b). Either way, we arrive at

$$N_\infty^2 \xi \hat{u}_{\Theta 0} - \xi \hat{u}_{\Theta 0 qq} - \frac{\xi}{q}\hat{u}_{\Theta 0 q} = 0 \qquad \Rightarrow \qquad \hat{u}_{\Theta 0} = A J_0(\beta q), \tag{47}$$

for some constant A. For large q this solution can be approximated by the standard Bessel function asymptotics:

$$\hat{u}_{\Theta 0} \approx A\sqrt{\frac{2}{\beta \pi q}} \cos\left(\beta q - \frac{\pi}{4}\right) \tag{48}$$

This now has to match with our outer solution in terms of R and y, which means that the outer must be:

$$\hat{u}_{\Theta 0} = \frac{\hat{u}_{2\infty}}{\sqrt{R}} \cos\left(\beta y + \frac{\pi}{4}\right) \qquad \text{and} \qquad A = \sqrt{\frac{\beta\pi}{2\delta}}\hat{u}_{2\infty}, \tag{49}$$

where $\hat{u}_{2\infty}$ is an arbitrary constant that will be set by matching with the solution inside the mean flow boundary layer. This also means that we may form a uniformly valid solution for $\hat{u}_{\Theta 0}$ outside the mean flow boundary layer,

$$\hat{u}_{\Theta 0} = \sqrt{\frac{\beta\pi}{2\delta}}\hat{u}_{2\infty} J_0\left(\frac{\beta r}{\delta}\right), \tag{50}$$

which agrees with both (47) and (49). Note also that, since $A = O(\delta^{-1/2})$, this outer solution acquires the largest amplitude, giving an overall contribution of $O(\epsilon^2/\delta^{5/2})$, near the centreline axis of the duct, a feature that can be seen in Fig. 7.

A similar argument may be followed for the temperature perturbation $\hat{T}_\Theta$. Equating equal power of δ in the energy equation (40e) gives

$$O(\delta^{-2}): \qquad \sigma^2 N_\infty^2 \hat{T}_{\Theta 0} - \hat{T}_{\Theta 0 yy} = 0 \tag{51a}$$

$$O(\delta^{-1}): \qquad \sigma^2 N_\infty^2 \hat{T}_{\Theta 1} - \hat{T}_{\Theta 1 yy} = \sigma^2 N_\infty^2 \hat{p}_{\Theta 0} - 2\hat{T}_{\Theta 0 Ry} - \tfrac{1}{R}\hat{T}_{\Theta 0 y} \tag{51b}$$

$$O(1): \qquad \sigma^2 N_\infty^2 \hat{T}_{\Theta 2} - \hat{T}_{\Theta 2 yy} = \sigma^2 N_\infty^2 \hat{p}_{\Theta 1} - 2\hat{T}_{\Theta 1 Ry} - \tfrac{1}{R}\hat{T}_{\Theta 1 y} + \hat{T}_{\Theta 0 RR} + \tfrac{1}{R}\hat{T}_{\Theta 0 R} - K^2\hat{T}_{\Theta 0} + \frac{\sigma^2}{\xi}T_{\mathrm{RHS}} \tag{51c}$$

with the leading order solution regular at the origin given by

$$\hat{T}_{\Theta 0} = \sqrt{\frac{\beta\sigma\pi}{2\delta}}\hat{T}_{2\infty} J_0\left(\frac{\beta\sigma r}{\delta}\right) \approx \frac{\hat{T}_{2\infty}}{\sqrt{R}} \cos\left(\beta\sigma y + \frac{\pi}{4}\right). \tag{52}$$

The last of the leading order solutions, $\hat{v}_{\Theta 0}$, may be found from equating equal powers in δ in the mass equation (40a), giving

$$O(\delta^{-2}): \qquad \hat{v}_{\Theta 0 y} + \mathrm{i}K\hat{u}_{\Theta 0} + \xi N_\infty^2(\gamma - 1)\hat{T}_{\Theta 0} = 0 \tag{53a}$$

$$O(\delta^{-1}): \qquad \hat{v}_{\Theta 1 y} + \mathrm{i}K\hat{u}_{\Theta 1} + \xi N_\infty^2(\gamma - 1)\hat{T}_{\Theta 1} = \xi N_\infty^2 \gamma \hat{p}_{\Theta 0} + \tfrac{1}{R}(R\hat{v}_{\Theta 0})_R \tag{53b}$$

$$O(1): \qquad \hat{v}_{\Theta 2 y} + \mathrm{i}K\hat{u}_{\Theta 2} + \xi N_\infty^2(\gamma - 1)\hat{T}_{\Theta 2} = \xi N_\infty^2 \gamma \hat{p}_{\Theta 1} + \tfrac{1}{R}(R\hat{v}_{\Theta 1})_R - P_{\mathrm{RHS}}. \tag{53c}$$

At leading order, $O(\delta^{-2})$, we may solve for $\hat{v}_{\Theta 0}$ to get

$$\hat{v}_{\Theta 0} = -\frac{\mathrm{i}K\hat{u}_{2\infty}}{\beta\sqrt{R}} \sin\left(\beta y + \frac{\pi}{4}\right) + \frac{\beta\xi(\gamma - 1)\hat{T}_{2\infty}}{\sigma\sqrt{R}} \sin\left(\beta\sigma y + \frac{\pi}{4}\right) + \bar{v}(R), \tag{54}$$

where $\bar{v}(R)$ is a slowly varying non-oscillatory term, similar in nature to $\bar{p}(R)$.

We now move on to the next order solutions from the $O(\delta^{-1})$ equations. Equation (43b) may be solved to give

$$\hat{u}_{\Theta 1} = B_1(R)e^{\mathrm{i}\beta y} + B_2(R)e^{-\mathrm{i}\beta y} + \bar{u}(R) \qquad \text{where} \qquad \xi N_\infty^2 \bar{u}(R) = \mathrm{i}K\bar{p}(R). \tag{55}$$

Using the same argument, equation (51b) may be solved to find

$$\hat{T}_{\Theta 1} = C_1(R)e^{\mathrm{i}\beta\sigma y} + C_2(R)e^{-\mathrm{i}\beta\sigma y} + \bar{T}(R) \qquad \text{where} \qquad \bar{T}(R) = \bar{p}(R). \tag{56}$$

Substituting in the now known solutions for $\hat{v}_{\Theta 0}$ and $\hat{u}_{\Theta 0}$ into the radial velocity equation at $O(\delta^{-1})$, equation (42b) gives

$$\hat{p}_{\Theta 1 y} = \bar{p}_R + \xi N_\infty^2 \bar{v} - (\gamma-1)\xi^2 N_\infty^2 \left(2 + \lambda - \frac{1}{\sigma^2}\right)\sigma\beta\frac{\hat{T}_{2\infty}}{\sqrt{R}}\sin\left(\beta\sigma y + \frac{\pi}{4}\right) \tag{57}$$

with solution

$$\hat{p}_{\Theta 1} = y\left[\bar{p}_R + \xi N_\infty^2 \bar{v}\right] + \bar{p}_1 + (\gamma-1)\xi^2 N_\infty^2 \left(2 + \lambda - \frac{1}{\sigma^2}\right)\frac{\hat{T}_{2\infty}}{\sqrt{R}}\cos\left(\beta\sigma y + \frac{\pi}{4}\right), \tag{58}$$

where $\bar{p}_1(R)$ is another non-oscillatory function of R independent of y. Avoiding the secular term $y[\cdots]$ which grows rapidly (i.e. linearly in $y = r/\delta$) implies that

$$\bar{p}_R + \xi N_\infty^2 \bar{v} = 0. \tag{59}$$

Finally, the $O(\delta^{-1})$ mass equation (53b) gives the solution for $\hat{v}_{\Theta 1}$. Similarly to the equation for $\hat{p}_{\Theta 1}$, in order to avoid a secular term in $\hat{v}_{\Theta 1}$ that grows linearly in y, the terms in (53b) independent of y must identically vanish. This leads to

$$\tfrac{1}{R}(R\bar{v})_R - \mathrm{i}K\bar{u} - \xi N_\infty^2(\gamma-1)\bar{T} + \xi N_\infty^2\gamma\bar{p} = 0 \tag{60}$$

Combining the derived equations for the non-oscillatory functions $\bar{u}$, $\bar{T}$, $\bar{p}$ and $\bar{v}$ from (55), (56), (59) and (60) gives the governing equation for $\bar{p}$

$$\bar{p}_{RR} + \tfrac{1}{R}\bar{p}_R + \left[(\Omega - MK)^2 - K^2\right]\bar{p} = 0, \tag{61}$$

which is exactly the wave equation expected in a uniform flow, with solution

$$\bar{p} = -D\frac{\mathrm{i}(\Omega - MK)}{\Lambda J_0'(\Lambda)}J_0(\Lambda R), \qquad \text{where} \qquad \Lambda^2 = (\Omega - MK)^2 - K^2, \tag{62}$$

where D is an arbitrary constant, and where $\bar{p}$ has been normalized so that $\bar{v}(1) = D$.

A. Summary

By using the Method of Multiple Scales, we have derived the leading order behaviour of the $O(\varepsilon^2)$ solution outside the mean flow boundary layer needed to match to the highly oscillatory solution within the boundary layer from section IV.B.1 when $N_\infty^2 < 0$ as $r \to 1$ and that satisfies the regularity conditions at the duct centreline $r = 0$. This solution is given by

$$\hat{T}_{O2} = \delta^{-5/2}\hat{T}_{2\infty}\sqrt{\frac{\beta\sigma\pi}{2}}J_0\left(\frac{\beta\sigma}{\delta}r\right) + O\left(\delta^{-1}\right) \approx \delta^{-2}\frac{\hat{T}_{2\infty}}{\sqrt{r}}\cos\left(\frac{\beta\sigma}{\delta}r - \frac{\pi}{4}\right) + O\left(\delta^{-1}\right) \tag{63a}$$

$$\hat{u}_{O2} = \delta^{-5/2}\hat{u}_{2\infty}\sqrt{\frac{\beta\pi}{2}}J_0\left(\frac{\beta}{\delta}r\right) + O\left(\delta^{-1}\right) \approx \delta^{-2}\frac{\hat{u}_{2\infty}}{\sqrt{r}}\cos\left(\frac{\beta}{\delta}r - \frac{\pi}{4}\right) + O\left(\delta^{-1}\right) \tag{63b}$$

$$\hat{v}_{O2} \approx \delta^{-1}\left[\frac{\mathrm{i}K\hat{u}_{2\infty}}{\beta\sqrt{r}}\sin\left(\frac{\beta}{\delta}r - \frac{\pi}{4}\right) - \frac{\beta\xi(\gamma-1)\hat{T}_{2\infty}}{\sigma\sqrt{r}}\sin\left(\frac{\beta\sigma}{\delta}r - \frac{\pi}{4}\right) + D\frac{J_0'(\Lambda r)}{J_0'(\Lambda)}\right] + O\left(1\right) \tag{63c}$$

$$\hat{p}_{O2} = -\delta^{-1}D\frac{\mathrm{i}(\Omega - MK)}{\Lambda J_0'(\Lambda)}J_0(\Lambda r) + O\left(1\right) \tag{63d}$$

where the approximations are valid away from $r = 0$. The constants $\hat{T}_{2\infty}$, $\hat{u}_{2\infty}$ and D are free to be matched to the inner solution within the mean flow boundary layer, as described in section IV.B.3.

References

[1] Petrie, O., and Brambley, E. J., "Nonlinear Acoustics in a Viscothermal Boundary Layer over an Acoustic Lining," *23rd AIAA/CEAS Aeroacoustics Conference*, American Institute of Aeronautics and Astronautics, Denver, 2017. doi:10.2514/6.2017-3376,.

[2] Brambley, E. J., "Acoustic implications of a thin viscous boundary layer over a compliant surface or permeable liner," *J. Fluid Mech*, Vol. 678, 2011, pp. 348–378. doi:10.1017/jfm.2011.116.

[3] Aurégan, Y., and Leroux, M., "Experimental evidence of an instability over an impedance wall in a duct with flow," *Journal of Sound and Vibration*, Vol. 317, No. 3, 2008, pp. 432–439. doi:10.1016/j.jsv.2008.04.020.

[4] Singh, D. K., and Rienstra, S. W., "Nonlinear asymptotic impedance model for a Helmholtz resonator liner," *Journal of Sound and Vibration*, Vol. 333, No. 15, 2014, pp. 3536–3549. doi:10.1016/j.jsv.2014.03.013.

[5] Eversman, W., "Effect of Local Impedance Variation and Non-Linearity on Multiple Tone Attenuation," *16th AIAA/CEAS Aeroacoustics Conference*, American Institute of Aeronautics and Astronautics, Stockholm, 2010. doi:10.2514/6.2010-3825,.

[6] Myers, M., "On the Acoustic Boundary Condition in the Presence of Flow," *Journal of Sound and Vibration*, Vol. 71, No. 3, 1980, pp. 429–434. doi:10.1016/0022-460X(80)90424-1,.

[7] Aurégan, Y., Starobinski, R., and Pagneux, V., "Influence of grazing flow and dissipation effects on the acoustic boundary conditions at a lined wall," *The Journal of the Acoustical Society of America*, Vol. 109, No. 1, 2001, pp. 59–64. doi:10.1121/1.1331678,.

[8] Eversman, W., and Beckemeyer, R. J., "Transmission of Sound in Ducts with Thin Shear Layers—Convergence to the Uniform Flow Case," *The Journal of the Acoustical Society of America*, Vol. 52, No. 1B, 1972, pp. 216–220. doi:10.1121/1.1913082,.

[9] Tester, B. J., "The Propagation and Attenuation of sound in Lined Ducts containing Uniform or "Plug" Flow," *Journal of Sound and Vibration*, Vol. 28, No. 2, 1973, pp. 151–203. doi:10.1016/S0022-460X(73)80102-6,.

[10] Rienstra, S. W., "A classification of duct modes based on surface waves," *Wave Motion*, Vol. 37, 2003, pp. 119–135. doi:10.1016/S0165-2125(02)00052-5.

[11] Brambley, E. J., "Fundamental problems with the model of uniform flow over acoustic linings," *Journal of Sound and Vibration*, Vol. 322, No. 4, 2009, pp. 1026–1037. doi:10.1016/j.jsv.2008.11.021.

[12] Brambley, E. J., "Well-Posed Boundary Condition for Acoustic Liners in Straight Ducts with Flow," *AIAA Journal*, Vol. 49, No. 6, 2011, pp. 1272–1282. doi:10.2514/1.J050723,.

[13] Renou, Y., and Auregan, Y., "On a Modified Myers Boundary Condition to Match Lined Wall Impedance Deduced from Several Experimental Methods in Presence of a Grazing Flow," *16th AIAA/CEAS Aeroacoustics Conference*, 2010. doi:10.2514/6.2010-3945,.

[14] Khamis, D., and Brambley, E. J., "The Effective Impedance of a Finite-Thickness Viscothermal Boundary Layer Over an Acoustic Lining," *21st AIAA/CEAS Aeroacoustics Conference*, 2015. doi:10.2514/6.2015-2229,.

[15] Khamis, D., and Brambley, E. J., "Viscous effects on the attenuation of a plane wave by an acoustic lining in shear flow," *J. Acoust. Soc. Am*, Vol. 141, No. 4, 2017, pp. 2408–2417. doi:10.1121/1.4979469,.

[16] Khamis, D., and Brambley, E. J., "Viscous effects on the acoustics and stability of a shear layer over an impedance wall," *J. Fluid Mech*, Vol. 810, 2017, pp. 489–534. doi:10.1017/jfm.2016.737,.

[17] Khamis, D., and Brambley, E. J., "Acoustics in a two-deck viscothermal boundary layer over an impedance surface," *AIAA Journal*, Vol. 55, No. 10, 2017, pp. 3328–3345. doi:10.2514/1.J055598,.

[18] Wu, X., and Luo, J., "Linear and nonlinear instabilities of a Blasius boundary layer perturbed by streamwise vortices. Part 1. Steady streaks," *Journal of Fluid Mechanics*, Vol. 483, 2003, pp. 225–248. doi:10.1017/S0022112003004233,.

[19] Dong, M., and Wu, X., "On continuous spectra of the Orr–Sommerfeld/Squire equations and entrainment of free-stream vortical disturbances," *Journal of Fluid Mechanics*, Vol. 732, No. 1760, 2013, pp. 616–659. doi:10.1017/jfm.2013.421,.

[20] Marensi, E., Ricco, P., and Wu, X., "Nonlinear unsteady streaks engendered by the interaction of free-stream vorticity with a compressible boundary layer," *Journal of Fluid Mechanics*, Vol. 817, 2017, pp. 80–121. doi:10.1017/jfm.2017.88,.

[21] Wu, X., "On generation of sound in wall-bounded shear flows: back action of sound and global acoustic coupling," *Journal of Fluid Mechanics*, Vol. 689, 2011, pp. 279–316. doi:10.1017/jfm.2011.416,.

[22] Wu, X., and Dong, M., "Entrainment of Short-Wavelength Free-Stream Vortical Disturbances in Compressible and Incompressible Boundary Layers," *Journal of Fluid Mechanics*, Vol. 797, 2016, pp. 683–728. doi:10.1017/jfm.2016.318.

[23] Landau, L. D., and Lifshitz, E. M., *Fluid mechanics*, Pergamon Press, 1987.

[24] Prangsma, G., Alberga, A., and Beenakker, J., "Ultrasonic determination of the volume viscosity of N2, CO, CH4 and CD4 between 77 and 300 K," *Physica*, Vol. 64, No. 2, 1973, pp. 278–288. doi:10.1016/0031-8914(73)90048-7,.

[25] Boluriaan, S., and Morris, P. J., "Acoustic Streaming: from Rayleigh to Today," *Int. J. Aeroacoustics*, Vol. 2, 2003, pp. 255–292. doi:10.1260/147547203322986142.

[26] Brambley, E. J., "Surface modes in sheared boundary layers over impedance linings," *Journal of Sound and Vibration*, Vol. 332, 2013, pp. 3750–3767. doi:10.1016/j.jsv.2013.02.028,.